Radar Systems and
Remote Sensing Laboratory

THE UNIVERSITY OF KANSAS CENTER FOR RESEARCH, INC.
2291 Irving Hill Road
Lawrence, Kansas 66045-2969

CORRECTION OF WINDSCAT SCATTEROMETRIC MEASUREMENTS BY COMBINING WITH AMSR RADIOMETRIC DATA

S. Song and R. K. Moore

Radar Systems and Remote Sensing Laboratory
Department of Electrical Engineering and Computer Science, University of Kansas
2291 Irving Hill Road, Lawrence, Kansas 66045-2969
TEL: 913/864-4835 * FAX: 913/864-7789 * E-MAIL: graham@ardneh.rsl.ukans.edu

RSL Technical Report 11960-1

June 1996

Sponsored by:

Oregon State University/NASA
Corvallis OR 07331-5503

Grant NS033A-04

Correction of WindScat Scatterometric Wind Measurements by Combining with AMSR Radiometric Data

Correction of WindScat Scatterometric Wind Measurements by Combining with AMSR Radiometric Data

I. Introduction

The wind vector on the ocean-surface can be determined from the measurements of radar backscatter of the ocean by utilizing a spaceborne scatterometer [1]. The global coverage, suitable spatial resolution, and frequent sampling allow the spaceborne scatterometer to provide wind data where it is otherwise unavailable [2]. However, the signal measured by the scatterometer is the representative from the sea surface only under clear sky conditions, or in the presence of light clouds. When heavy clouds and precipitation are present, the signal received at the scatterometer is reduced because of the attenuation by clouds and rain. Accurate determination of the sea-surface wind vectors requires estimation of this reduction and corrections in the wind retrieval process.

The concept of using radiometric measurements to make correction on the scatterometric data was presented in [3]. A correction process was developed to evaluate the atmospheric attenuation from SMMR brightness temperature for the SEASAT satellite scatterometer [4,5].The results showed the correction appeared to improve the accuracy of wind vector determination for some situations. Our previous report [6] described work done on the correction algorithm for the SeaWinds scatterometer measurements by combining with the AMSR data. Different cloud distributions were considered and the seed-growing method was used to simulate the distribution. The correction utilized an iteration procedure to combine the radiometric measurements with the scatterometric measurements and corrected the attenuated sea backscatter. The simulation results

showed the wind speed errors after correction are small for most cases. For simplicity, the correction was performed only for overlapping and partial over-lapping of one scatterometer cell by two or three radiometer cells. The collocation of actual scatterometer measured points with actual radiometer measured points was not considered because too little information was available. The actual geometry of the scatterometer and the radiometer, combined with the satellite motion, will determine the measured point locations. The spatial distribution of the scatterometer cells and the radiometer cells will be quite complex. For a specific scatterometer measurement, the collocation of these two kinds of cells is needed to determine which radiometer measurement can be used for the correction.

Another important problem is the wind direction. We assumed the scatterometer looked upwind in the correction algorithm presented in the last report. This meant only the magnitude of the wind vector was considered. Obviously, such an assumption will influence the correction accuracy. When the true wind direction approaches the crosswind direction, the result will be worse.

Here we present the original correction algorithm with emphasis on the three improvements: the collocation of the two kinds of measurements, the consistence with the general SeaWind Algorithm [7] and the wind direction. For actual geometry of the SeaWind scatterometer and the AMSR radiometer, the collocation of AMSR data to the scatterometer data is performed by using the triangle method proposed in [7]. Different cloud distributions are simulated using the seed-growing method. The brightness temperature on one AMSR cell is averaged to provide the radiometer data for that point (center of the cell). The brightness temperature at the scatterometer measured point is obtained by weighting or interpolation from the collocated radiometer points. The correction algorithm was also revised to meet the

requirements of the main SeaWind Algorithm.The data structure is consistent with the general SeaWind Algorithm. At the same time the interfaces needed for the connection with the main algorithm were also considered. The consideration of wind direction was carried out by two steps.First we evaluated the errors caused by assuming upwind. Then, an alternative was developed to derive the wind direction of the current cell from the previous cells. The influence of this procedure on the correction results was also analyzed.

We then developed a simplified correction algorithm. When we dealt with the wind direction problem in the correction algorithm, we found that, if we get rid of the wind retrieval part, we will not need to make a wind direction assumption. This can be done by using the wind speed from the previous wind-vector cell to obtain the surface brightness. Thus, we can get two benefits. One is that the correction algorithm is simplified and less time needed for one iteration. The other is that the interface to the main SeaWinds Algorithm is simplified. The disadvantage of the simplified algorithm is that the correction will not converge to the exact solution because the wind speed is not included in he iteration. However, as long as the wind retrieval part in the main SeaWinds Algorithm can get accurate wind speed, the simplification will not cause much degradation in correction performance.

For both original and simplified correction algorithms, we give simulations of performance for different cloud distributions , different wind speeds and different scatterometer points. The simulation results show that both of them give obvious improvements in the wind retrieval.

II. Collocation of Scatterometer Measurements and Radiometer Measurements

The SeaWinds Scatterometer is a Ku-Band radar. The scatterometer has two antenna beams at different elevation angles scanning conically.The conical scan design represents a change from the fixed fan-beam antennas of previous NASA spaceborne scatterometers (SeaSat and NSCAT). This changes the locations of the measurements. The two incident angles are 40 and 46 degrees. As the planned orbit height is about 800 km, the conical scan of the outer beam (elevation angle 46 degrees) will produce a radar measurement swath width up to 900 km on each side of the satellite track. The inner beam (elevation angle 40 degrees) produces a swath width up to 700 km. The sea surface from 200 to 700 km off track will be considered the primary swath of the SeaWind instrument because the greater number of azimuth measurements will improve the wind

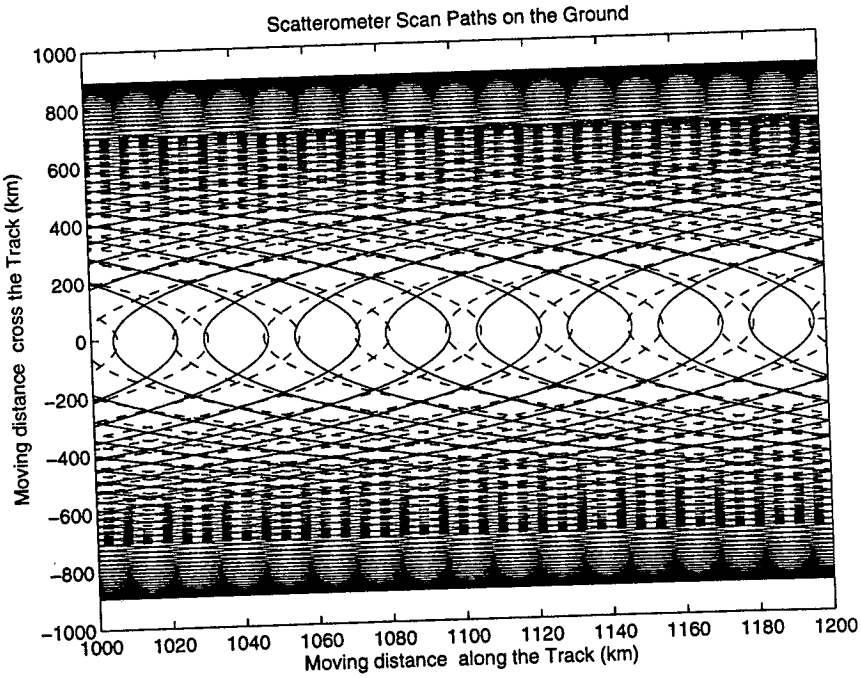

Fig. 2-1. Scatterometer scan paths on the sea surface

retrieval performance. The scan paths of the two beams on the ground are shown in Fig.2.1. The scan period is 3.75 seconds. With the beam widths of 1.6 and 1.4 degrees separately for the two beams, the two way radiation half power width on the ground is about 25 km by 40 km. The satellite speed will be 6.6 km/s; therefore the along-track spacing of σ_0 samples will be approximately 25 km. From Fig. 2-1, we can see that many fewer samples will be available near the center of swath than near the edge. The number of measured points (samples) on the sea surface will influence the attenuation correction results.

The Advanced Microwave Scanning Radiometer (AMSR) has six frequency bands:6.6, 10.65, 18.70, 23.80, 36.50 and 89.00 GHz. It also uses conical scan, but only part of the scan circle is used for sampling. The scan swath is predicted as 1720 km. The scan period is

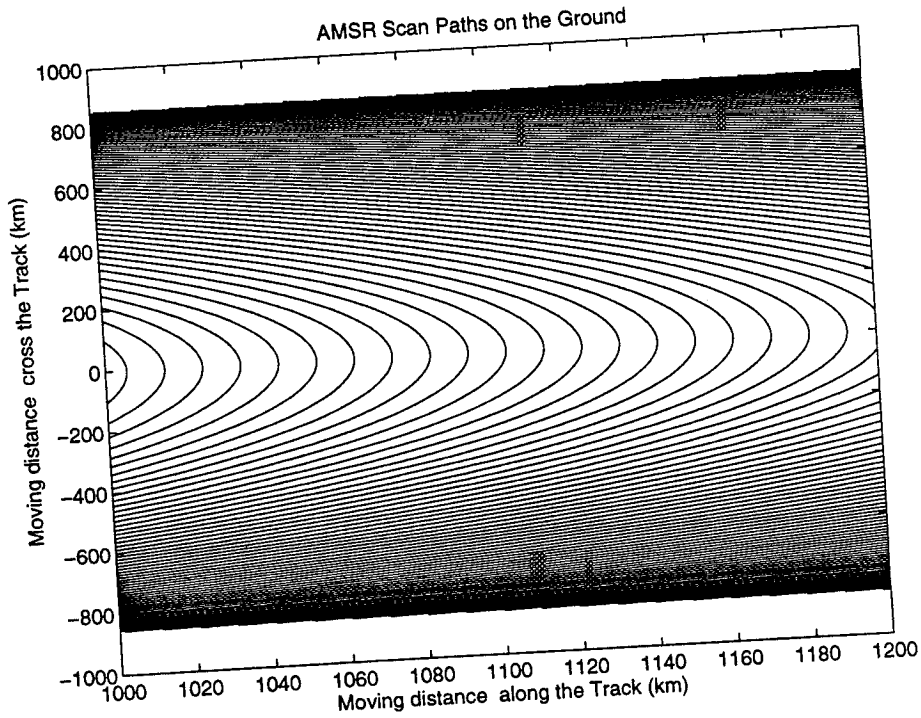

Fig. 2-2 AMSR scan paths on the sea-surface

1.49 seconds (40.3 rpm). The pointing angle is 46.7. Considering the geometry of the earth, the incident angle is about 55 degrees. The spatial sampling interval is 10 km by 10 km. The frequency we used for attenuation correction is 18.70 GHz. At this frequency, the beam widths in two directions are the same (0.65 degrees). The foot prints on the sea surface are about 25 km by 15 km and thus the spatial resolution is about 25 km by 25 km. The scan paths on the sea surface of the AMSR are shown in Fig. 2-2. From the figure we know that the smaller number of measured points (samples) for AMSR at the center region of swath may influence the correction performance because the collocating process has to use some AMSR points farther from the scatterometer point we are trying to correct.

Fig. 2-3 gives two examples of the measured-point distributions of scatterometer and AMSR in a region in the size of the wind-vector cell (50 km by 50 km). The wind-vector cell

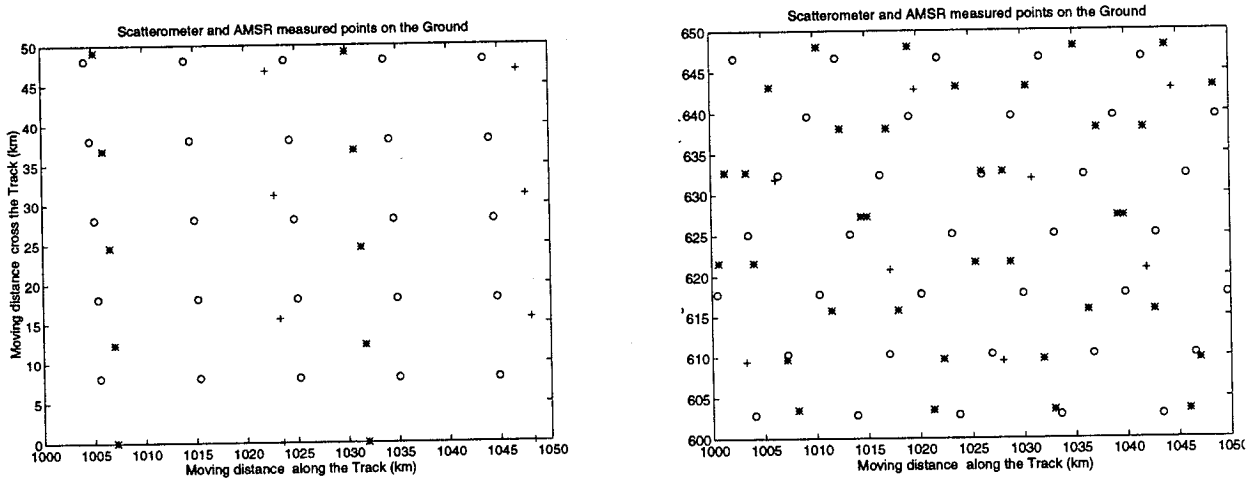

(a) Central wind vector cell (b) Edge wind vector cell

Fig. 2-3 Measured points in the wind vector cells
(+ for beam 1 and * for beam 2 of Scatterometer; o for AMSR)

in Fig. 2-3(a) is located at the central region of the swath and Fig. 2-3(b) near the edge. From

the two figures we see that the measured points of the scatterometer are different in number (density) and distribution (locations) . However, the measured points of AMSR are not changed very much and show some regularity.

From above, we know that few scatterometer measured points are coincident with AMSR measured points. However,when we do the attenuation correction, we need the brightness temperature (T_b) at the σ_0 point. Thus, to get the T_b, we have to choose some AMSR measured points near the scatterometer measured point. This process is collocation. We utilize the triangle-scheme proposed in [7] to collocate the measured points on the sea surface. However, before collocation, we need to sort the measured points of the two instruments and store the points in three dimensions. The first two dimensions are the cell index (I,J) for the cell size 25 km by 25 km.The third dimension is the depth of the cell, actually, the number of measured points in that cell.We use K to denote the third index. After the sorting, we select several T_b points which are closer to the σ_0 point than other T_b points. If we pick up three T_b points for one σ_0 point,

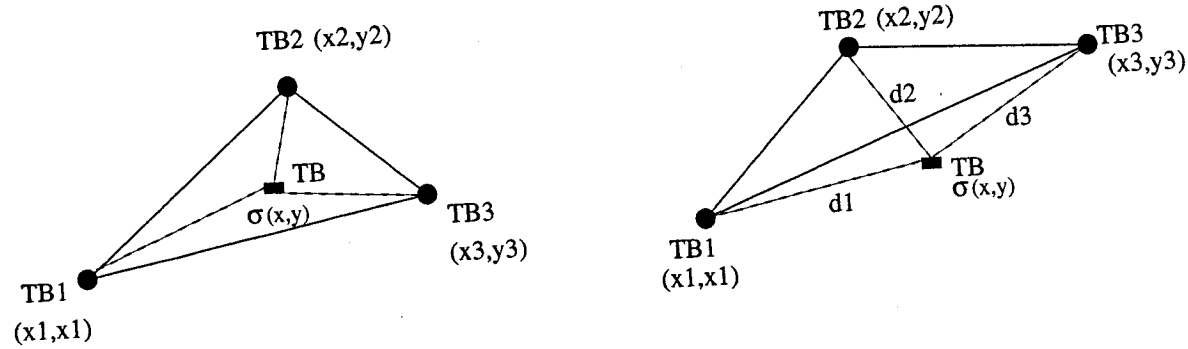

Fig. 2-4 Collocation by the triangle scheme

it is the triangle scheme. The selection is performed by searching the T_b points in the cells of

index (I,J) to (I+1,J+1).Considering the AMSR's space sampling interval is 10 km by 10 km, there always exist some T_b points in this area.Actually, from the analysis of geometry of AMSR measured points, we found there are at least four T_b points in one 25 km×25 km cell.

As long as the collocated points are found,the triangle scheme can be used to obtain the brightness temperature at the σ_0 point by interpolation or weighting depending on the relative location of the σ_0 point and the three T_b points. This is shown in Fig. 2-4, where T_{bi}(i=1,2,3) are the brightness temperatures measured by AMSR at the corresponding points and σ_0 is the measurement of the scatterometer at that point. The six lines connecting the four points give four triangles. The three T_b points (T_{bi}, i=1,2,3) made the big triangle. Lines from the point to the three T_i points give three small triangles. If the area of the big triangle is equal to the sum of the area of the three small triangles, then we say that the σ_0 point is inside the triangle; otherwise the σ_0 is outside the large triangle. For a triangle with vertices at (x_1,y_1), (x_2,y_2) and (x_3,y_3), its area s can be obtained by

$$S=\frac{1}{2}|d_{x1}\cdot d_{y2}-d_{x2}\cdot d_{y1}| \qquad (2-1)$$

where $d_{x1}=x_2-x_2$,$d_{x2}=x_3-x_1$,$d_{y1}=y_2-y_1$,and $d_{y2}=y_3-y_1$.

If the σ_0 point is inside the triangle, the T_b value at the σ_0 point can be obtained by interpolation[7]

$$T_b=ax+by+c \qquad (2-2)$$

where x and y are the coordinates of the σ_0 point. The coefficients a,b and c came from following equations

$$\begin{aligned} x_1 a + y_1 b + c &= T_{b1} \\ x_2 a + y_2 b + c &= T_{b2} \\ x_3 a + y_3 b + c &= T_{b3} \end{aligned} \qquad (2\text{-}3)$$

where T_{bi} (i=1,2,3) are the three brightness temperatures at the corresponding points (x_i, y_i) with i=1,2,3. For a σ_0 point which is not inside the triangle, we use weighting to calculate the T_b value at this point, which is

$$T_b = d\left(\frac{T_{b1}}{d_1} + \frac{T_{b2}}{d_2} + \frac{T_{b3}}{d_3}\right) \qquad (2\text{-}4)$$

where d_1, d_2, and d_3 are the distances of the σ_0 point to the three T_i points respectively. d depends on these distances and is calculated by

$$d = \frac{d_1 d_2 d_3}{d_1 d_2 + d_1 d_3 + d_2 d_3} \qquad (2\text{-}5)$$

For the weighting formula (2-4), when the T_b is in a uniform distribution ($T_{b1}=T_{b2}=T_{b3}=T_{b0}$), the T_b calculated at the σ_0 point is also T_{b0}. When the σ_0 point is at the same distance to the three T_b points, its T_b value will be the average of T_{b1}, T_{b2}, and T_{b3}.

III. The Cloud and Rain Distribution

The brightness temperature (T_b) used for correcting the attenuation on the σ_0 is calculated by the collocation method from three AMSR measurements at different locations. Thus,the distribution of clouds and rain will affect both the value of T_b and the value of σ_0 . When we evaluate the attenuation of the clouds, we may define the cloud distribution by using two terms, the magnitude and the size. The magnitude is a measure of the cloud thickness and rain rate in the cloud. The size is a two dimensional factor for each rain cell. The contours of magnitude inside the cell form the cloud (rain) distribution.

As mentioned in the previous report [6], the correction should be performed only for heavy clouds, which include rain. For clear sky or thin cloud, there is no need to do the correction, for the attenuation will be negligible. This means the correction algorithm performance depends on the cloud distribution. However, at the time we do the correction, we have too little information to figure out the magnitude of the clouds. We need to find some method to determine if the correction is needed, because the correction algorithm is located before the wind retrieval part in the structure of the SeaWind Algorithm presented in [7]. It is preferred to make the correction algorithm fit that structure.

The concept of excess temperature used in attenuation correction, presented by Moore and Ulaby [3], can be used to make the decision by combining some knowledge of sea-surface condition. First, we analyze the brightness temperature measured by AMSR. Fig. 3-1 shows the contributions to the measured brightness temperature, which includes the sea-surface emission, atmospheric emission and reflected sky components. The sea-surface emission Tb is attenuated by L and denoted by Ts. The other two terms comprise the excess temperature Tex, denoting the amount by which the measured apparent temperature exceeds the sea surface contribution.

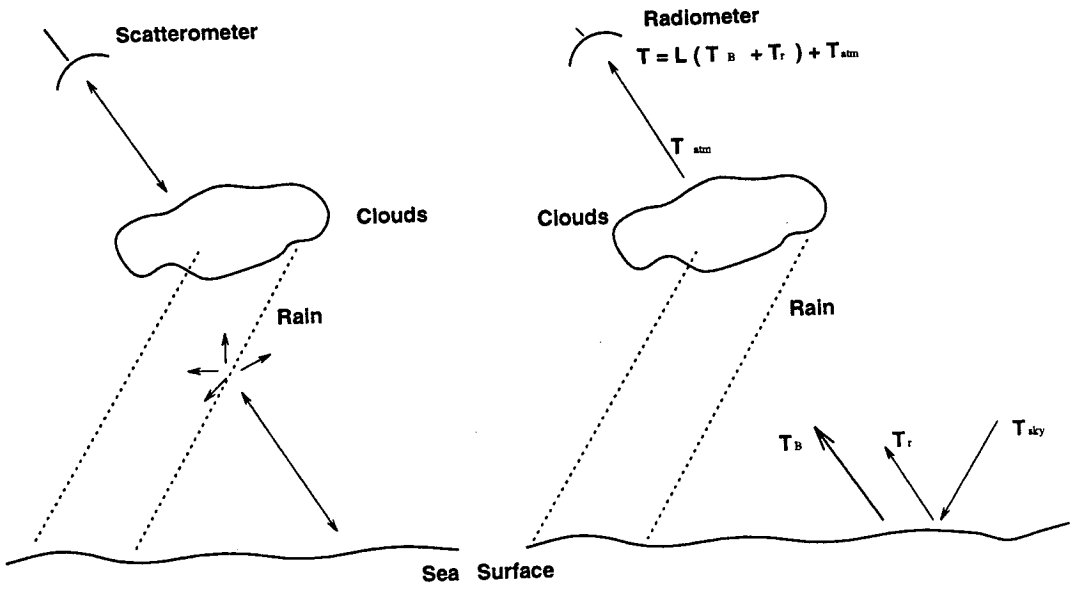

Fig. 3-1. The components of the measured apparent temperature

The attenuated sea surface brightness temperature T_s is [8]

$$T_s = (82 + 1.06u)\, e^{-\alpha} \qquad (3\text{-}1)$$

where u is the wind speed on the sea surface and α (nepers in 3-1) is the attenuation factor which depends on the excess temperature T_{ex} by the cubic relation [9]

$$\alpha\ (dB) = AT_{ex} + BT_{ex}^2 + CT_{ex}^3 \qquad (3\text{-}2)$$

where A, B, and C are empirical coefficients. This equation gives attenuation at 14.6GHz. We need to scale it to the frequency of AMSR used for correction, 18.7GHz. Then

$$\alpha_{AMSR}(dB) = \alpha\ (dB)\ \left(\frac{18.7}{14.6}\right)^2 \qquad (3\text{-}3)$$

So, the α in (3-1) will be

$$\alpha\,(nepers) = \frac{\alpha_{AMSR}(dB)}{8.686} \qquad (3-4)$$

The measured T_b is the sum of sea surface contribution and the excess temperature.

$$T_m = T_s + T_{ex} \qquad (3-5)$$

Fig. 3-2(a) shows the measured T_m versus the excess temperature T_{ex}. The measured T_m does not always increase with excess temperature because attenuation cause the sea surface contribution to decrease as the excess temperature increases.The decision to use the correction is performed by comparing the measured T_m to a set threshold. The threhold depends on the amount of attenuation we can tolerate.For easy understanding, we translate the attenuation to the relative error of σ_0 between the measured and the true σ_0 . Fig. 3-1(b) shows the error versus excess temperature.

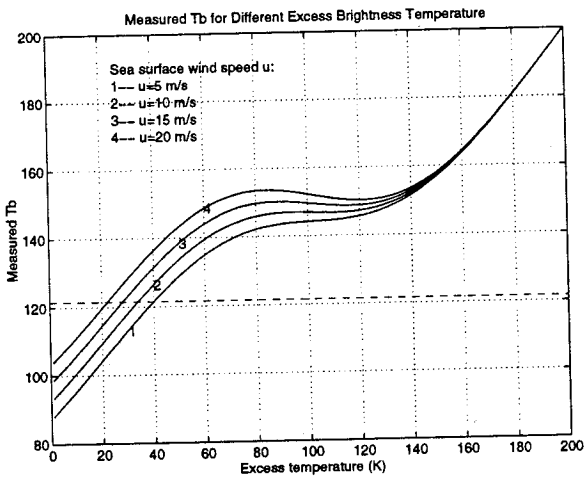

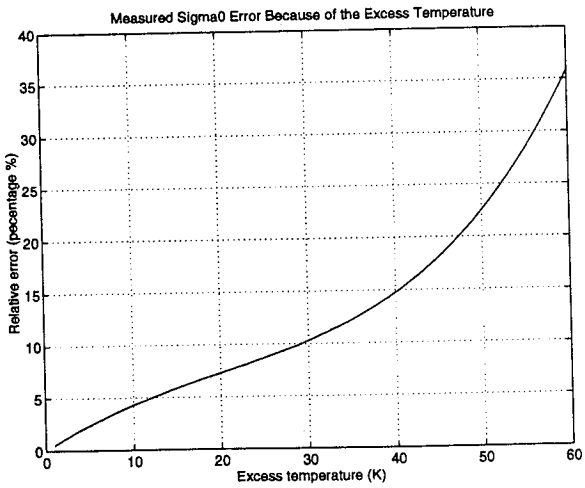

(a) Measure T_m vs. T_{ex} (b) Relative error in percentage

Fig. 3-2 Measured T_m, excess temperature T_{ex} and the error caused by attenuation

From Fig. 3-2, we can set the threshold on T_m if we know how much error on σ_0 we can tolerate. That is, from the threshold on σ_0 error we get the threhold on the excess temperature T_{ex} from Fig. 3-2(b) and then get the threshold on T_m from Fig. 3-2(a). However, it will be better to relate the threshold to the wind speed, because the same percent error on σ_0 will cause different errors on the wind-speed retrieval. Fig. 3-3 gives the wind-speed errors caused by the different percent errors in σ_0 for two wind speeds, 10m/s and 20 m/s at different azimuth angles.

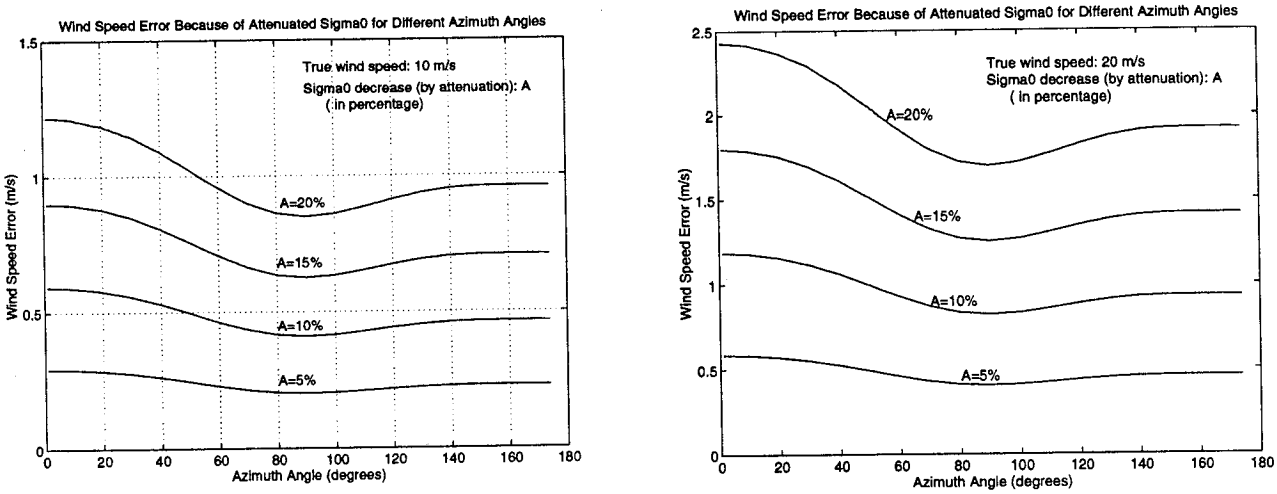

(a) Erorr for true wind 10m/s (b) Error for true wind 20m/s

Fig. 3-3 Wind speed error caused by different attenuation on Sigma0

From the figure, we observe that for 15% attenuation of σ_0 the maximum wind speed error approaches 1 m/s for true wind speed 10m/s, but 2 m/s for true wind speed 20m/s. Considering that the performance requirement on wind speed for the SeaWind instrument is an error of 2 m/s and the fact that other errors sources may exist such as noise and interference, it is necessary to correct when the wind speed error caused by attenuation is between 1m/s to 2 m/s. This corresponds to the attenuation of σ_0 of about 10% to 15% which corresponds to excess temperature in the range of 30 K to 40 K. From Fig. 3-2(a), we find the threhold on the

measured Tm should be located near 120 K. If the threshold is set too low, we may waste time in data processing. If the threhold is set too high, we may get too large an error on wind speed. This is a trade-off on the SeaWind requirements.

After determining the excess temperature, we can simulate different distributions of clouds for the correction algorithm. We consider two cases: stratiformcase and convective storms. For the stratiform rain, we assume uniform distribution in thickness and presence over a large square area of specified size. For the convective case, the seed growing method [6] is used to simulate the distribution,but with a little modification on the spatial distribution function. The original distribution function was

$$T_{ex}=T_{peak}e^{-(\frac{r}{r_0})^2}$$

where T_{peak} is the peak value at the center of cloud or rain cell. r_0 determines the fall off rate. T_{ex} is the excess temperature at the distance of r. The contours with this distribution are circles. To simulate a more complex cloud or rain profiles, we modify it to the form

$$T_{ex}=T_{peak}e^{-(\frac{x^2}{r_{0x}^2}+\frac{y^2}{r_{0y}^2})}$$

where r_{0x} and r_{0y} are the decay distances in the x-axis and y-axis directions, respectively. This distribution function incorporates the natural cell asymmetry [9]. Fig. 3-4 shows several example distributions of excess temperature inside one wind-vector cell with different numbers of storms and fall off rates. The locations and the peak temperatures for different storms are randomly distributed.

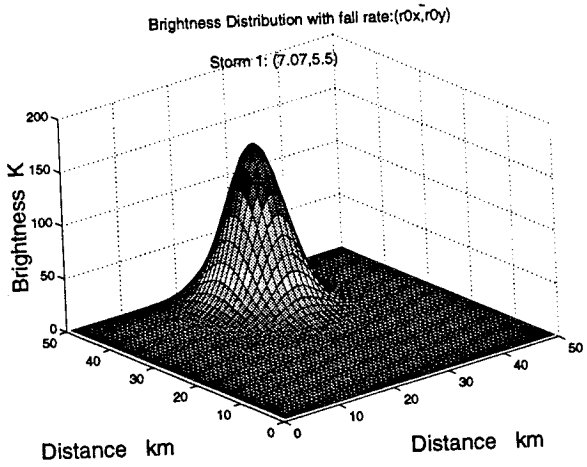

(a) One storm case

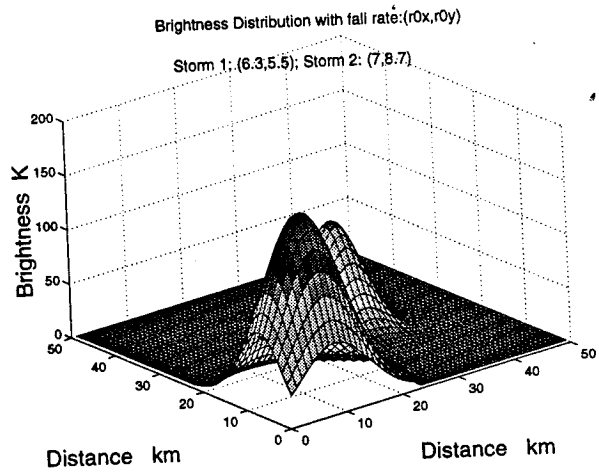

(b) Two storm case

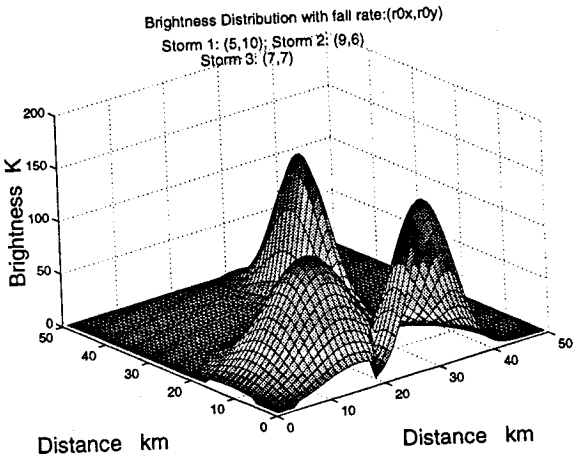

(c) Three storm case

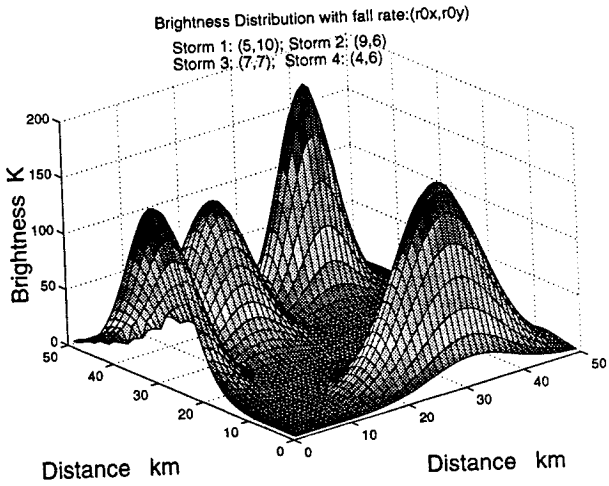

(d) Four storm case

Fig.3-4 Cloud distribution for different fall rates and peaks

The measured temperature by AMSR is the average temperature over one AMSR cell. To calculate the average value, we divide the AMSR measurement cell into sub-cells. The temperature in each sub-cell is calculated using the distribution function given above. The formula used in last report [6] is rewritten bellow

$$T_{m\text{-}subcell} = T_{ex\text{-}subcell} + T_s e^{-\alpha\ subcell}$$

where $T_{m\text{-}subcell}$ is the measured temperature in the subcell. $T_{ex\text{-}subcell}$ is the excess contribution to that subcell. T_s is the surface temperature and its contribution to that subcell will be attenuated by the attenuation in that subcell. A similar formula exists for the scatterometer measurements. By averaging over all the subcells inside one measurement cell, we can get the simulated measurement, which is the apparent temperature for AMSR and the σ_0 for the scatterometer.

IV. The Correction Algorithm Based on Scattering

The correction algorithm estimates the attenuation by combining the radiometric data and the scatterometric data and then removing the attenuation effect from the measured σ_0. The algorithm is implemented through an iteration process [6]. In this section, we deal with some specific implementation problems of the algorithm, which include the wind direction assumption, the maximum iteration times and the interface with the SeaWind Algorithm. We first give a brief view of the correction algorithm and then treat these problems in more detail.

4.1 The correction algorithm

The correction algorithm is an iterative process. We use steps to illustrate this process.

Step 1. Scatterometer and Radiometer geometry.

In this step, the necessary geometric parameters will be given as input from the SeaWinds Algorithm of JPL. This is because the locations and the angles will be needed for the attenuation calculation.(*INTERFACE NEEDED)*

Step 2. Initialization.
Set the required values for the parameters used in the correction algorithm, which include

1) Set the minimum required improvement of one iteration
2) Set the maximum number of iterations.
3) Set initial estimate (guess) of sea surface wind speed (U_{bias} normally 10 m/s) and direction.
4) Assume no attenuation at the first step

Step 3. Calculate the sea surface contribution to brightness temperature by using

$$TB_{bias} = 1.06\ U_{bias} + \varepsilon_s\ T_w \quad (K)$$

where

ε_s = surface emissivity of water (=0.53) for H polarization
T_w = water surface temperature (assumed 290 K);
U_{bias}= estimated wind speed (m/s);

Step 4. Calculate the Excess Brightness Temperature

1) First obtain the apparent temperature TB_{avg} measured by the radiometer from the main SeaWind Algorithm (*INTERFACE NEEDED)*

2) Then calculate the excess temperature from the measured and the estimated values

$$T_{bex} = T_{bavg} - T_{bbias}$$

Step 5. Use cubic model for attenuation to calculate the attenuation in dB

$$\alpha_{cub\_dB}(\theta) = A_1 T_{ex} + A_2 T_{ex}^{\ 2} + A_3 T_{ex}^{\ 3}$$

where A_1 ,A_2 and A_3 are empirical constants. Tex is the excess temperature estimated in the last step (T_{bex}).

Step 6. Frequency Scaling

The frequency used by the Scatterometer is 13.4 GHz. For the AMSR, the data we used for correction is at 18.7 GHz. The cubic model is valid for 14.6 GHz. The estimated attenuation factor α needs to be scaled to the proper frequencies by

$$\alpha_{scat\_dB} = \alpha_{cub\_dB} \times (13.4/14.6)^2$$

$$\alpha_{rad\_dB} = \alpha_{cub\_dB} \times (18.7/14.6)^2$$

Step7 . Correction of the Measured σ_0

1) Obtain the scatterometer measured σ_0 from the main SeaWind Algorithm (*INTERFACE NEEDED)*

2) Change the attenuation factor α in dB to α in nepers

$$\alpha_{scat\_np} = \alpha_{scat\_dB} / 8.686$$

$$\alpha_{rad\_np} = \alpha_{rad\_dB} / 8.686$$

3) Correct the measured σ_0

$$\sigma^0_{corr} = \sigma^0_{measured} \exp(2\alpha_{scat})$$

Step 8. Estimate the Sea Surface Wind from the corrected σ_0

$$U_{est} = 10^{\frac{\alpha_{corr}(dB) - 10G}{10H}}$$

Where G and H are from the SASS model function. During actual implementation, the Model Function used by the main SeaWind Algorithm can be used here. We still have the problem on wind direction. Possible solutions include

1) Assume upwind and accept errors in T_{bias} from this.
2) Use output of alias-removal Seawinds algorithm; this could have large errors if several footprints have attenuation. Must rerun during iterations.
3) Use direction from previous measurement cell.

Detailed discussion and results for these solutions are to be given later.

(INTERFACE WITH THE WIND RETRIEVAL PART OF THE MAIN SEAWIND ALGORITHM FROM JPL IS NEEDED, IF SOLUTION ONE IS NOT USED.)

Step 9. Evaluate the correction

1)Compute the difference of estimated sea surface wind speed in the last two iterations

$$\Delta U = | U_{est(i)} - U_{est(i-1)} |$$

2) ΔU is the improvement of the correction in the step i compared with step i-1

3) Either of following two conditions will stop the iteration:
   a. ΔU < required improvement

b. iteration number exceeds the set maximum number

4) If neither condition satisfied , continue the correction procedure

Step 10. Calculate the new sea surface temperature contribution

$$T_{b\_bias} = [\ 1.06 \times U_{bias} + \varepsilon_s T_w\ ]\ \exp(-\alpha_{rad})$$

where α_{rad} is the new estimated attenuation factor for the radiometer measurement.

Step 11. Go to step 4 and repeat the correction until the set conditions are satisfied

The flow chart of the correction algorithm is given on the next page. The diagram shows that the correction is made on the basis of a σ_0 cell. That mean the correction is applied successively to σ_0 cells, one by one. The geometric parameters needed for correction are specified for the σ_0 cell that is going to be corrected. The knowledge of the sea surface conditions may be obtained from other sources.

The diagram also shows several interface blocks. These interfaces work as input and output gates through which the correction algorithm obtains the needed data from the main SeaWind Algorithm , and at same time sends out the data it processed. The first three interfaces can be made into one part, depending on the structure of the main SeaWind Algorithm. The fourth interface is a two way gate that may utilize the Wind Retrieval part of the main SeaWind Algorithm, but it will depend on the wind direction consideration discussed later. The fifth interface is purely an output gate for the processed data. The details of these interfaces are to be presented later.

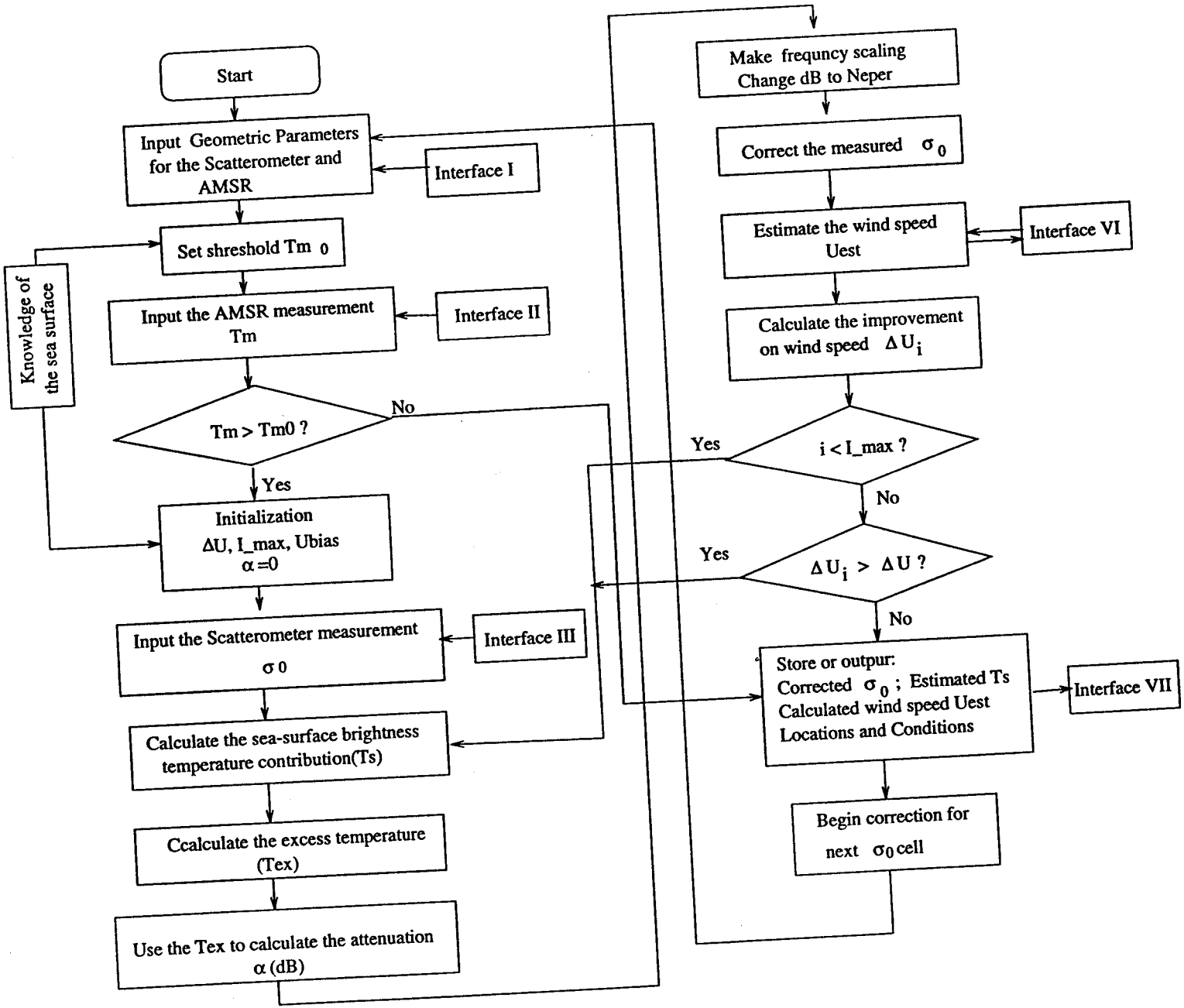

Flow Chart of the Correction Algorithm

4.2 The wind direction in the correction algorithm

In the correction algorithm, the sea surface contribution to the AMSR measurements is needed in every iteration. The surface contribution depends on the sea surface wind speed estimated in that iteration. The wind speed is obtained by implementing the Model Function (G & H) which is selected depending on the wind direction. Thus, inaccurate information on the wind direction will cause an error in the estimation of wind speed and the sea surface contribution. For this problem, we have three possible solutions:

1) Assume upwind direction.

2) Use the direction from the Wind Retrieval Algorithm in the main SeaWind Algorithm.

3) Use previous cell wind direction.

The second solution could perform well, but it needs the Wind Retrieval Algorithm to operate at each iteration. There are two difficulties with this. One is that the structure of SeaWind Algorithm is not compatible with such an arrangement. The other is that the correction time will be dramatically increased because the Wind Retrieval Algorithm is quite complex. Thus, we only consider the first and the third solution.

Fig. 4-1 gives some simulated results for the stratiform cloud distribution. The wind direction used in correction is first assumed as the true wind direction, as shown in Fig. 4(a). Then, the direction used in correction is assumed to deviate from the true wind direction as shown in Fig. 4(b) - Fig. 4(d), From these results, we see that, for all direction assumptions,

the correction algorithm gives obvious improvement comparing over the uncorrected results. However, larger deviations from the true direction will result in less improvement. When the deviation is 90°, the performance is the worst. Because of the symmetry of the SASS model function between [0, 90] degrees and [180, 90] degrees, the improvement at 45 degrees is similar to that at 135 degrees. Because of these errors,, the third solution for wind direction is better than the first. This is because the previous cell wind direction usually tends to be much closer to the true wind direction in the current cell than the assumed upwind direction.

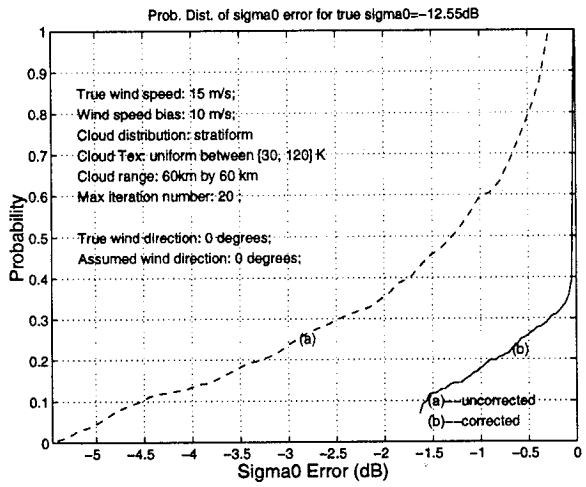

(a)

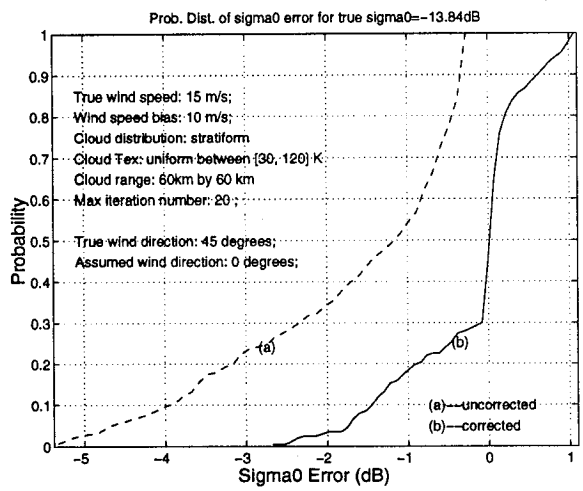

(b)

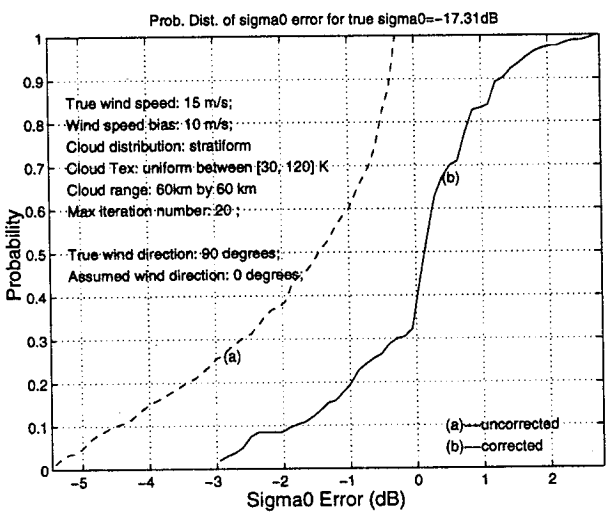

(c)

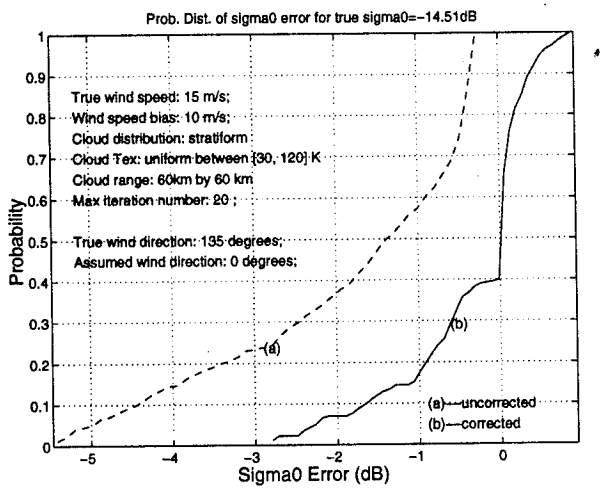

(d)

Fig. 4-1 The σ_0 error for stratiform clouds

For convective storms, the wind direction influence on the correction results is not as obvious as that for stratiform clouds. Fig. 4-2 shows the corrected results for this case. Fig. 4-2(a) ,Fig. 4-2(b) and Fig. 4-2(c) are only different in the assumed wind direction . Fig. 4-2(d) is the same as Fig. 4-2(b) except for different true wind speeds. From these simulated results we see that no big difference exists between different wind direction assumption. However, from Fig. 4-2(c), we see that if the assumed wind direction is far from the true direction, the corrected results have larger error. This is similar to the case for stratiform clouds (see Fig. 4-1(c)). It implies that a poor wind direction assumption may cause large errors.

The simulation results show that the third solution for direction assumption is the best one. If the wind direction is not available for the previous cell, the first solution may be used but with somewhat degraded performance.

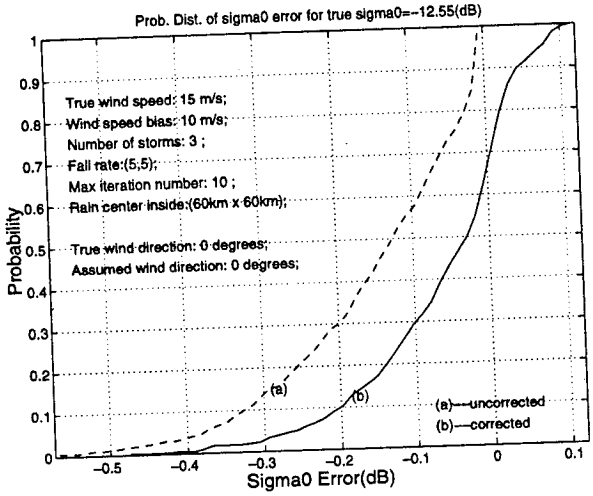

(a)

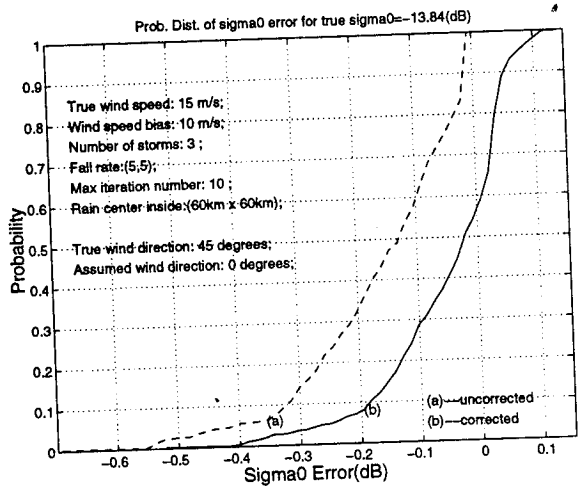

(b)

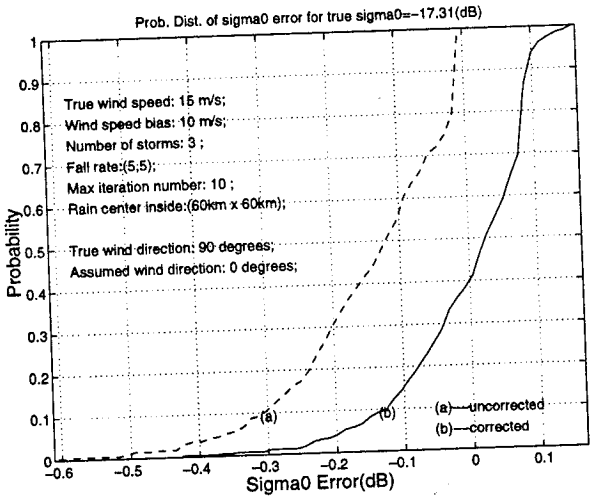

(c)

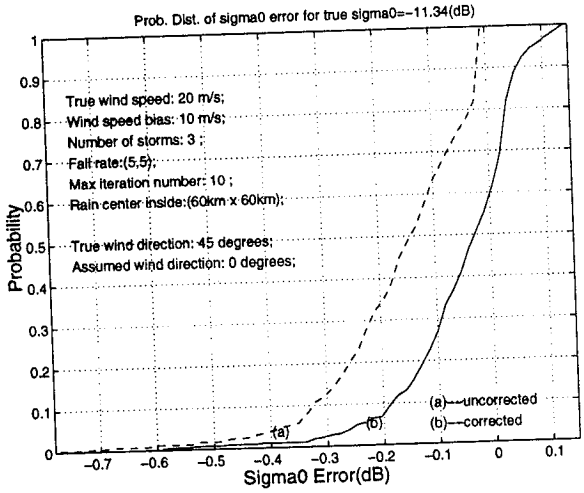

(d)

Fig. 4-2 The σ_0 errors for convective clouds

4.3 The number of iterations required

In the correction algorithm, two parameters control the end of iteration. One is the required improvement for one iteration and the other is the maximum iteration number. The required improvement can be determined by the accuracy requirement. The maximum iteration number depends on the wind speed and cloud distribution. For different excess temperatures, the iteration numbers required to achieve the same level of error after correction are different. Fig. 4-3(a) shows the statistical results. It is a histogram of iteration number versus the excess temperature T_{ex}. The true wind speed is assumed as a Gaussian distribution with a mean of 15 m/s and a standard deviation of 5 m/s. The excess temperature is uniformly distributed between 50 K to 200 K. The figure shows that for same level of error requirement, the number of iteration needed is maximum for excess temperatures in the range 80 K to 150 K. At extremely high excess temperature, the number of iterations becomes less. This mean that iteration converges faster in this range. This phenomena can be explained by Fig. 3-2(a).We replot it as Fig. 4-3(b) for easy comparison. In this figure, the relation of measured temperature versus excess temperature can be divided into three segments. The first segment is a linear segment with obvious sea surface wind contribution. The second segment is a non-linear segment with smaller sea-surface contribution. The third segment is again linear but with little sea surface contribution. We know the correction algorithm is a process to solve several equations from given measured data by iteration. The solution should be the excess temperature (or attenuation). Thus a linear relation between the knowns and unknowns will make the iteration converge faster than a non-linear relation with small or negative slope.

That is, fewer iterations will be needed for the linear region, shown in Fig. 4-3(a), even though the third segment has very high attenuation.

Combining Fig. 4-3(a) and (b), we can determine the maximum iteration number needed for the correction algorithm. This can be done by only observing the measured AMSR data, Tm. If the Tm is less 140 K, the maximum iteration number can be set to less than 8. If the Tm is higher than 160 K, the maximum iteration number can be selected between 8 and 15. If Tm is in the non-linear region, 140 to 160, the iteration number should be set larger than the linear cases. From Fig. 4-3(a), it needs at least 15 iterations. We suggest it should not exceed 25. One reason for this is that too much time may be needed for a large number of iterations. The other reason is that too many iterations may cause the algorithm to converge to a n erroneous value, especially for the case of an inaccurate wind direction assumption (as shown in Fig. 4-1).

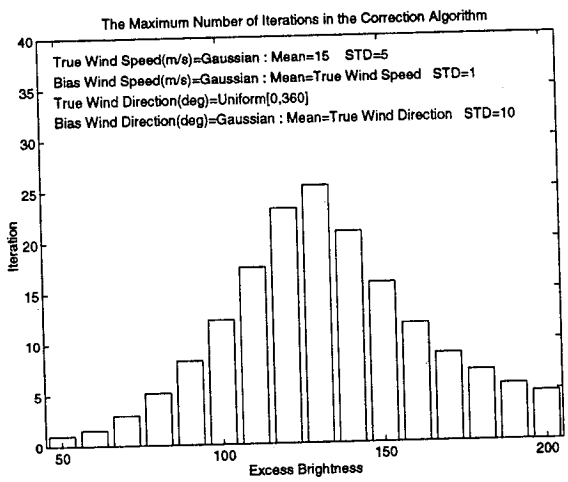

(a)

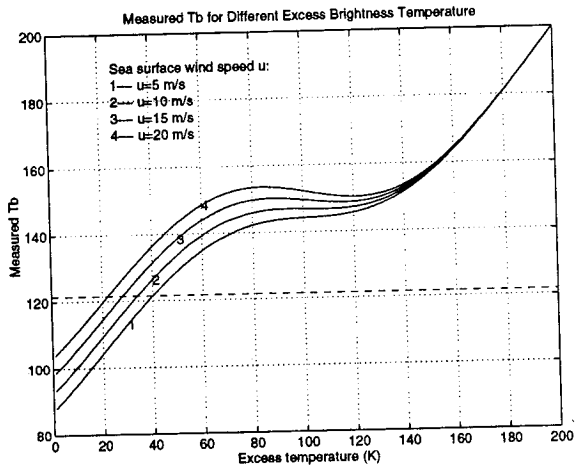

(b)

Fig. 4-3 Maximum iteration number and excess temperature

4.4 Interfaces of the correction algorithm to the SeaWind Algorithm

The correction algorithm is one part of the main SeaWinds Algorithm, so it must fit to the main algorithm. Fig. 4-4 show the blocks of σ_0 and T_b resampling module, the correction algorithm and the wind retrieval modules.. The σ_0 and T_b resampling module will perform the collocating of the scatterometer data and AMSR data. After finding the AMSR data corresponding to the scatterometer data, the correction algorithm is entered. The output of the correction algorithm will be corrected Sigma0. After the Sigma0 is regrouped into the wind-vector cell , the wind retrieval-module is entered to calculate the wind speed and direction from the corrected Sigma0.

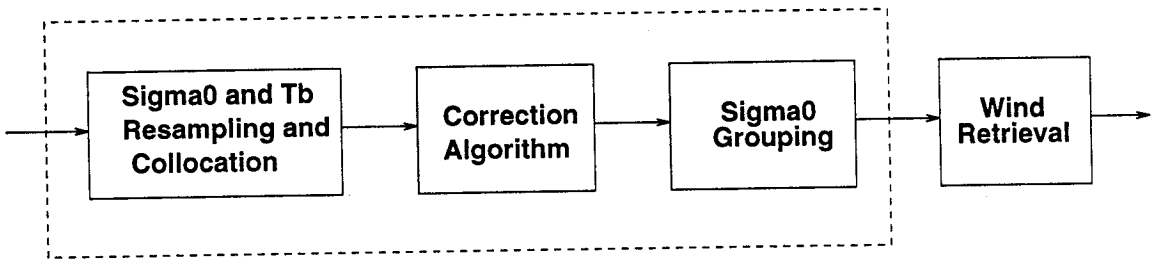

Fig. 4-4 The blocks of data resampling, correction and wind retrieval

The wind retrieval module and correction algorithm work with different cell sizes. The wind retrieval-module calculates the wind speed and direction in the wind vector cell (50 km by 50 km). The correction algorithm does correction for a σ_0 cell (25 km by 25 km). The wind-retrieval module needs the σ_0 values from multiple σ_0 points because the correction is performed separately for each σ_0 measurement. Hence the corrected σ_0 should not go directly to the wind retrieval module. Fig. 4-5 shows where the correction algorithm is

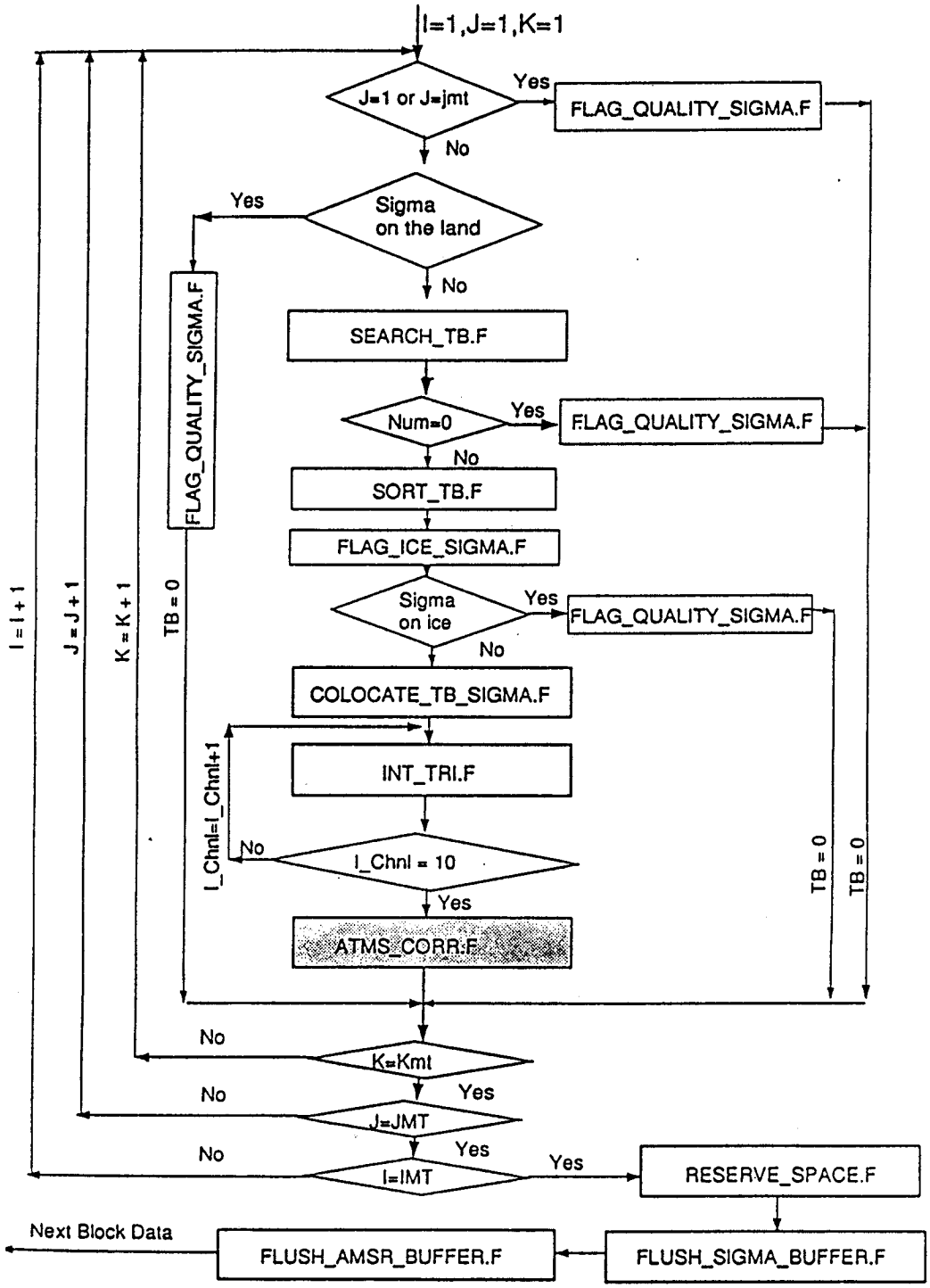

Fig.4-5 The location of the correction algorithm in the main SeaWinds Algorithm[7]

located in the JPL SeaWinds Algorithm [7]. This figure shows that the correction algorithm is inside the Resampling Module. That is, the correction is first performed and the corrected σ_0 is stored. After all corrections for σ_0 data are finished, then the corrected σ_0 data go to the wind-retrieval module. If we were to use values from the wind-retrieval algorithm, this would have to change and the wind retrieval part would become an iterative process.

Thus, the first three interfaces shown in the blocks of the correction algorithm (Fig. 4-1) can be combined to one interface which serve as an input to the correction algorithm. It is the input interface The third interface would only be used with method 2 which we discussed. The fourth interface will be the same as specified in Fig. 4-1 as an output port for the corrected data.

Besides the input σ_0 and T_b, some parameters must be input to the correction algorithm. These include global parameters and local parameters. Global parameters are the values which are the same for all σ_0 cells. The local parameters are the values specified for the current σ_0 cell. Following are the parameters :

Global Parameters:

Incident angles (for two beams).

Local parameters:

Locations (X and Y coordinates)

Sea-surface wind estimate

The output will be the corrected σ_0 with the corresponding T_b and parameters. The correction algorithm includes the model function from SASS. If it utilizes the model function used in the wind retrieval part, another interface is needed.

V. Simulation of the Correction Algorithm Based on Scattering

To evaluate accurately the performance of the correction algorithm, the simulation of the correction algorithm was performed under the conditions specified in the SeaWinds Algorithm. In simulation, the specified SeaWinds geometry was used to calculate the measured points for both scatterometer and AMSR. Different cloud distributions were created and used to evaluate the statistical results. The collocating technique [7] was used to avoid assuming any specific overlapping or partial overlapping for the scatterometer measured cells and AMSR measured cells. Because the measured data for the SeaWind instrument are unavailable, the measured data was simulated. After correction, the evaluation was performed by comparing the corrected σ_0 with true σ_0 or using it to calculate the wind speed. Fig. 5-1 shows the blocks of simulation steps.

The correction is performed on the σ_0 data block by block, as specified in Fig. 4-5. In one data block, the correction is performed on its σ_0 point . The σ_0 value on one point is denoted by index (I,J,K), where I is the index cross track direction and J is the index along track direction. K is the index denoting the number of the σ_0 points in one cell (25 km by 25 km). Fig. 5-2 illustrates the geometry and location of the correction performed. The inner beam (beam 1) of the scatterometer has a swath of 700 km on one side. The outer beam (beam 2) has a swath of 900 km on one side. The swath on one side for the AMSR is about 860 km. Beyond this swath, there is no radiometer data. The primary swath of the SeaWinds instrument is from 200 to 700 km from the track. Then the simulation was performed inside the 700 km swath on both sides of the track.

In simulation, two types of cloud and rain distribution are used: stratiform and convective. For stratiform rain, uniform distribution is assumed. For convective storms individual cells are assumed. The quadratic exponential distribution is used to describe each storm. Statistical properties of the clouds and rain are simulated by the seed growing method [6].

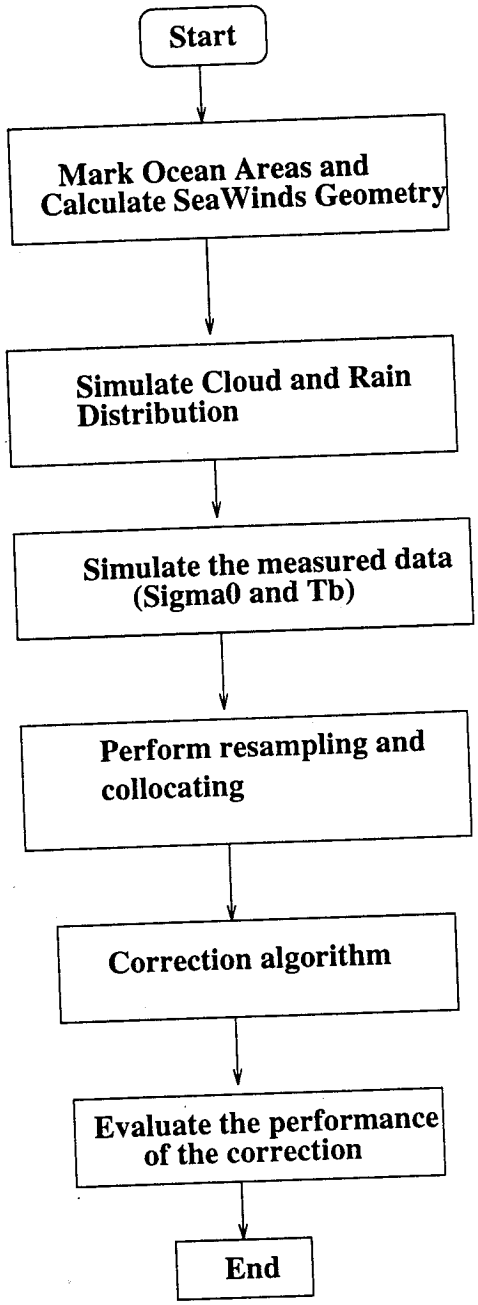

Fig.5-1 Blocks of the Simulation Process

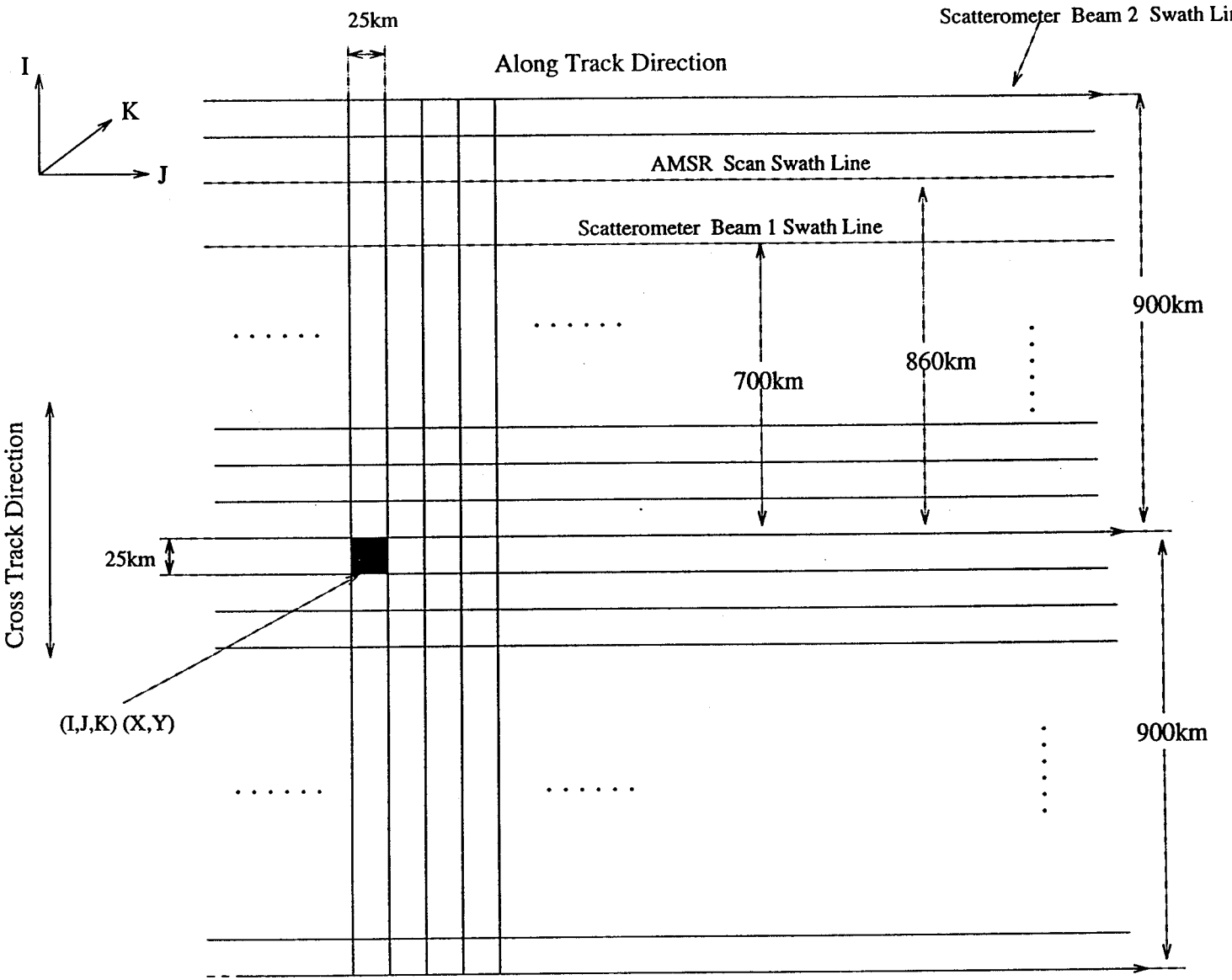

Fig.5-2 Geometry and locations of corrected cells

The measured data were obtained by simulation. That is, first , the true values were calculated and then modified to account for the attenuation from the simulated clouds and rain. The attenuation is different at different locations because of the cloud distribution (for convective storms). The simulated measurements are the average values over the scatterometer or AMSR footprint. For simplicity, we assume the foot prints are all rectangular.

The output of the correction algorithm is the corrected σ_0 . To evaluate the performance of the correction algorithm, we define a parameter, called improvement, which is the difference of the error between corrected and uncorrected results. This parameter is used for both σ_0 and wind speed. Because it is easy to see the performance using wind-speed error, wind speed error is calculated even though it is not the output of the correction algorithm. When calculating the wind-speed error, we assume the wind direction is known. No big difference is expected if the wind retrieval algorithm in the main SeaWinds Algorithm can get the wind direction from multi-point σ_0 values.

Simulation was performed for several different cases. Section 4.2 showed the simulated results for different direction assumptions. Section 4.3 showed simulation performed for different iteration numbers. To evaluate the correction algorithm in more detail, simulation results of the correction performance are shown for comparison in following four situations:

a. comparison for stratiform clouds and convective clouds;

b. comparison for different cloud distributions for convective clouds;

c. comparison for different σ_0 locations relative to the collocated Tb points;.

b. comparison for different sea surface wind speeds.

As discussed in section IV, choosing the previous-cell wind direction for the current cell bias gives better results than other solutions. In simulation, this method is used. Previous cell wind direction is simulated by a Gaussian distribution with a mean equal to the current cell wind direction and a standard deviation equal to 10 degrees.

The maximum iteration number used in the correction algorithm comes from comparing Fig. 4-3(a) and Fig. 4-3(b). For measured temperature in the range [0, 140] K, the maximum iteration number is set to 8. For measured temperature in the range [140, 160] K, the maximum

iteration number is 20. For measured temperature in the range [160, Max] K,the maximum iteration number is 10. For final implementation of the correction algorithm, we may have more segments or even use an interpolation formula to get the maximum iteration number.

a. Comparison of performance in stratiform and convective form clouds;

Some results on the performance of the correction algorithm for stratiform and convective clouds were already given in section 4.2 in Fig. 4-1 and Fig. 4-2. Other results are shown in Fig. 5-3. The first two plots are σ_0 improvement and the third and fourth plots are wind- speed improvement, The simulation conditions for these results are for corrected point (I,J,K)=(40,5,4), where I and J are the cell index and K is the point index in that cell. The true wind speed is 15 m/s and wind speed bias is 10 m/s. The cloud excess temperature is set as a uniform distribution in [30, 120] K. For stratiform clouds, the cloud range is a square of 60 km by 60 km. For convective clouds, the centers of all storms are inside a square of size 60 km by 60 km. The simulated results show that the improvement obtained by the correction is much greater for stratiform cloud than for convective storms. For stratiform clouds, the correction algorithm will converge to the exact solution if enough iterations are performed. For convective clouds, it will not converge to the exact solution because of the effects of averaging attenuation on both σ_0 and Tm. The correction algorithm has better performance for large attenuations. This is actually an advantage of the correction algorithm, because we need more improvement when higher attenuation occurs.

b. Comparison of performance for different cloud distributions for convective clouds;

Fig. 5-4 shows the results of correction for different numbers of storms within the simulation area. The storms are characterized by their excess temperature. The distribution of the excess temperature for each storm is quadratic-exponentially distributed. The peaks were randomly picked between 80 K to 200 K. The fall-off rate is set from input. The center of each storm was randomly located inside a square area of size 60 km by 60 km. The simulation was

performed at point (I,J,K)=(60,7,8). The conditions are true wind speed =15 m/s, wind speed bias=10 m/s, and fall-off rate=(5,5). The figures show that, for different numbers of storms, the correction algorithm always gives obvious improvement. The larger the number of storms, the more the improvement obtained.

c. Comparison of performance for different σ_0 locations relative to the collocated Tb points

When we made the above comparisons, each simulation result was at a σ_0 point. Now, we analyze the influence of different σ_0 points (or locations) on the correction performance. Considering there are so many different locations of σ_0 and T_b, it is impossible to simulate every situation. A simple method is used to show the general trend as shown in Fig. 5-5(a). A σ_0 point is selected and after collocation, we get the collocated three T_b points. Then, we move the σ_0 away from its original location. The "*" is used to denote the σ_0 point. The "o" is used for Tb. We see the selected σ_0 point is originally inside the triangle formed by three T_b points and located very close to one T_b point. For the different σ_0 locations, Fig. 5-5(b) gives the simulation results. The best performance for these cases is obtained when the σ_0 point is located at the original place. This is reasonable because at this point the σ_0 cell and Tb cell are almost coincident. After the σ_0 point is moved away, the results become worse. If the σ_0 point is too far away from the collocated T_b points, there is little improvement obtained from the correction, as for location 5 in the figure. Fortunately, this will rarely happen for the SeaWind instruments. We can see this from Fig. 2-3 in section II, where the distance from any σ_0 point to its collocated three T_b points can not exceed 15 km in either edge wind-vector cell (the best case) or central wind-vector cell (the worst case). This mean the σ_0 point can not go beyond the location 3 in Fig. 5-5(b). Therefore, the influence of different σ_0 locations will not be very strong. The simulation results already shown in this report support this conclusion.

d. comparison of the performance for different sea surface wind speeds.

Finally, we compare the performance of the correction algorithm for different sea-surface

wind speeds. Fig. 5-6 shows the simulation results for sea-surface wind speeds of 10 m/s and 20 m/s in both stratiform clouds and convective clouds. The simulation conditions are shown in the figure. From the results, we see that for both cases, the correction gives obvious improvement. For lower sea surface wind speed, the maximum number of iterations can be set smaller to save correction time.

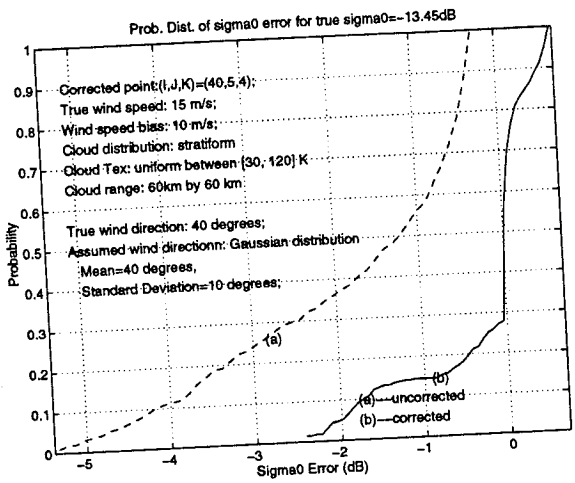

(a) σ_0 error for stratiform clouds

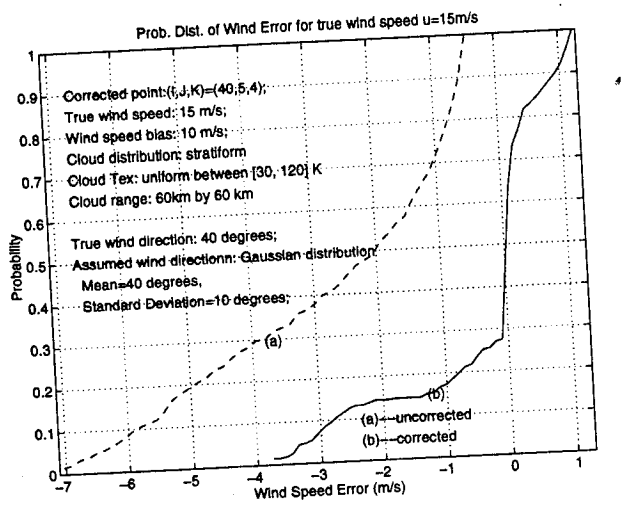

(b) Wind speed error for stratiform clouds

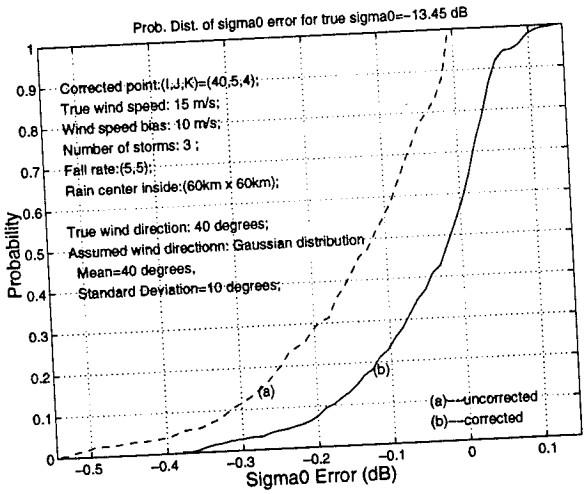

(c) σ error for convective clouds

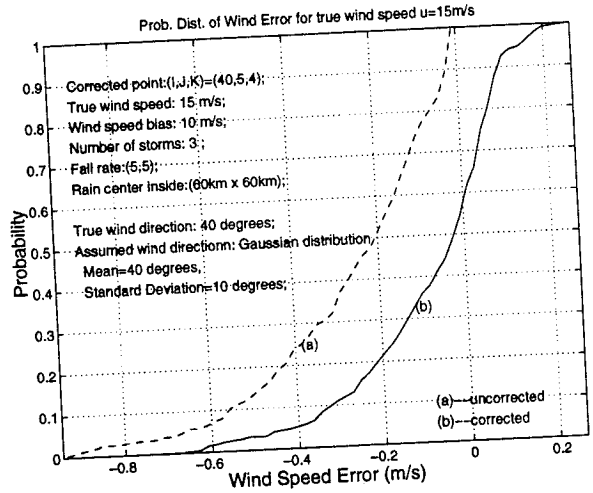

(d) Wind speed error for convective clouds

Fig. 5-3 Comparison of correction performance for two forms of clouds

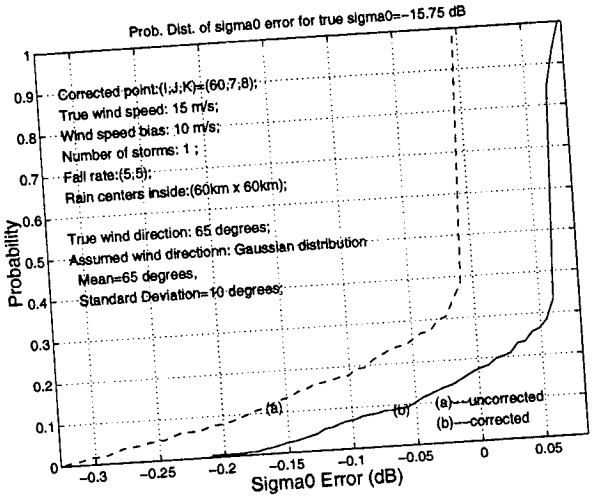

(a) One storm

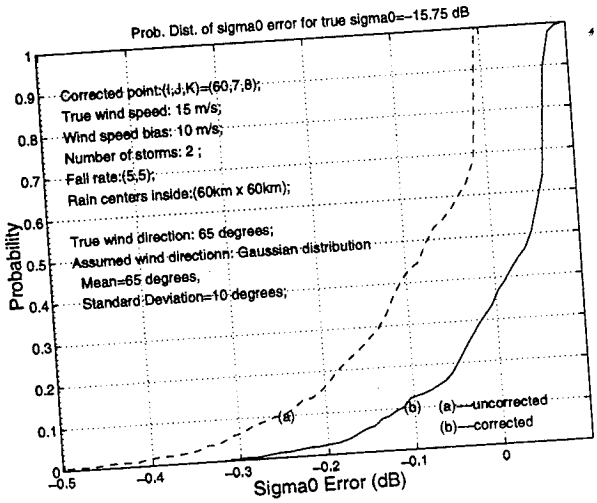

(b) Two storms

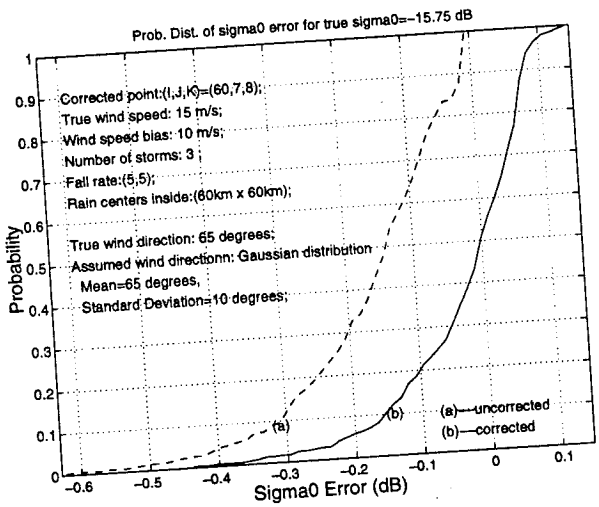

(c) Three storms

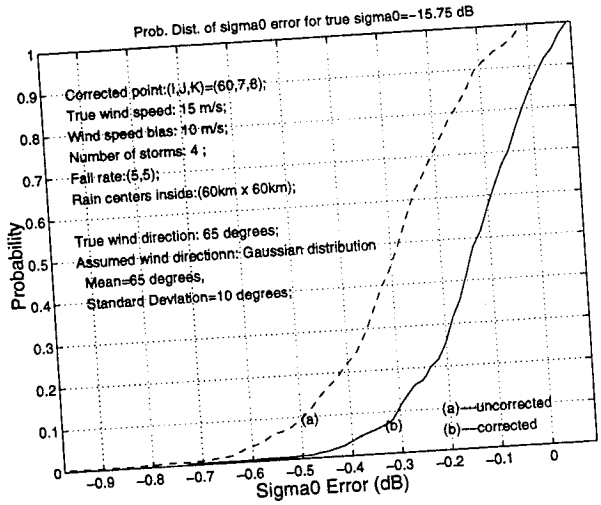

(d) Four storms

Fig. 5-4 Correction performance for different number of storms

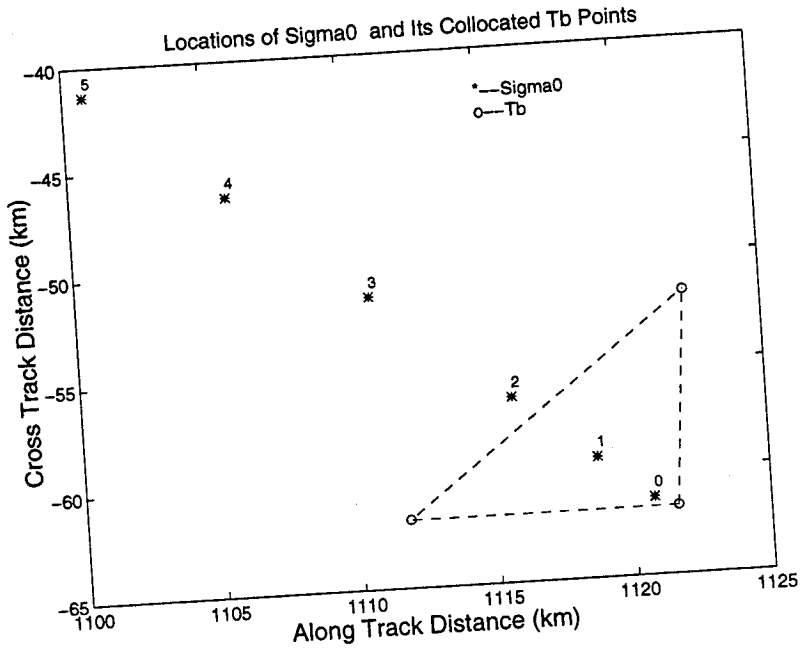

(a) σ_0 locations

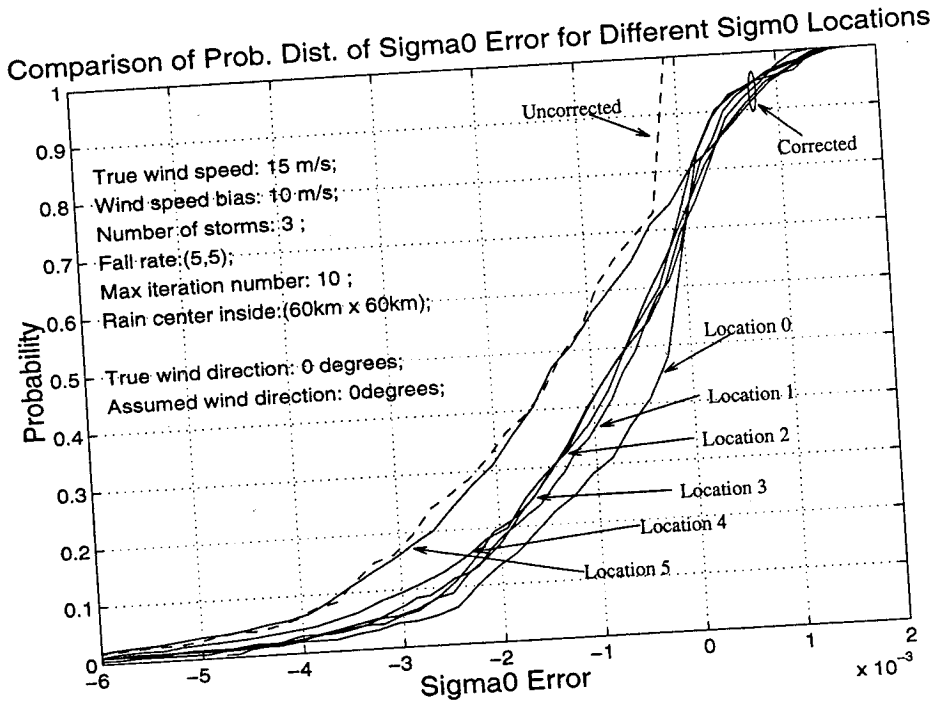

(b) σ_0 error

Fig. 5-5 Influence of the locations of σ points on correction performance

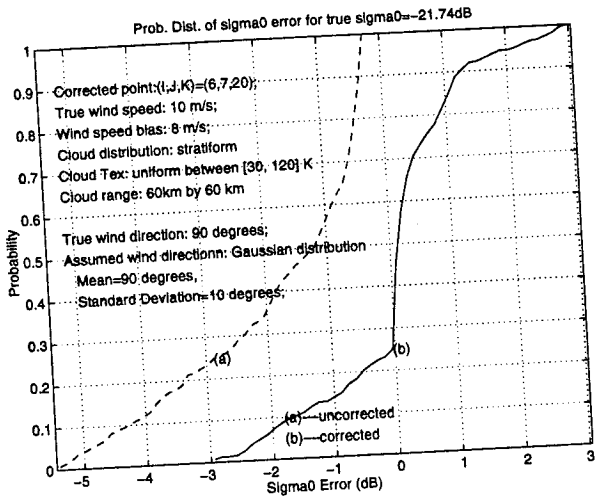

(a) Wind speed = 10 m/s and stratiform clouds

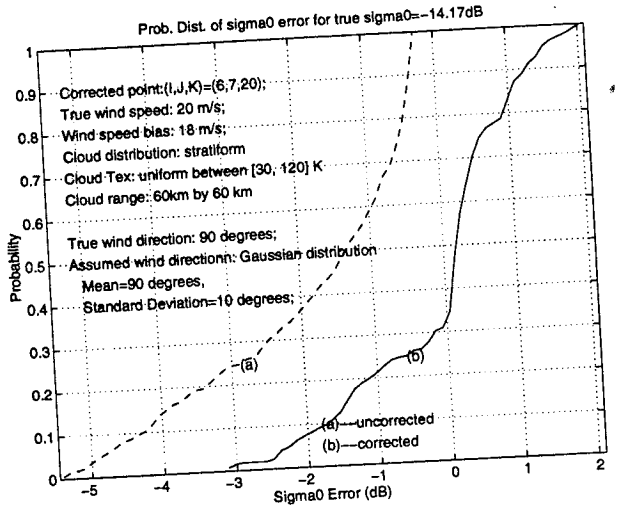

(b) Wind speed =20 m/s and stratiform clouds

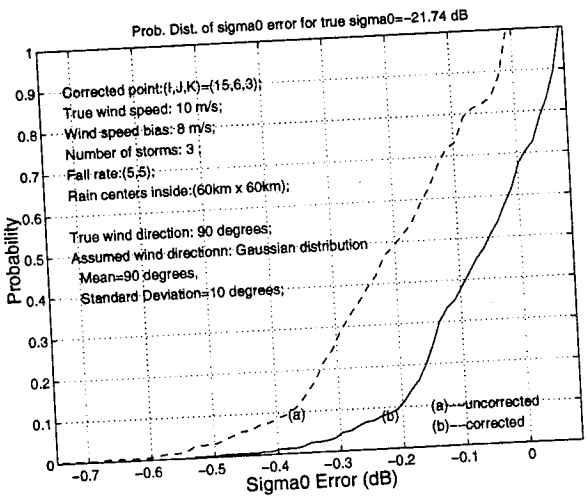

(c) Wind speed = 10 m/s and convective clouds

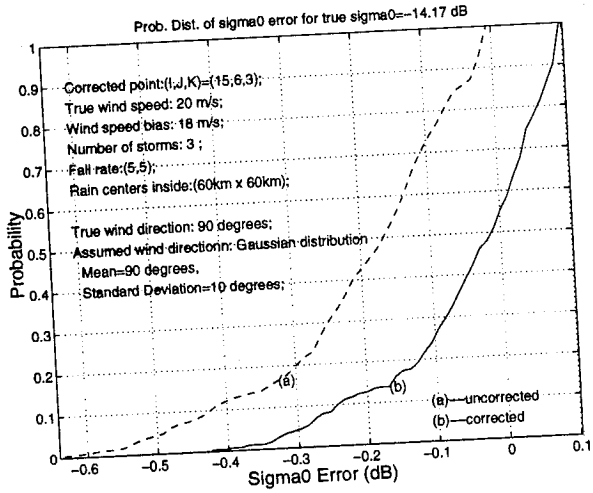

(d) Wind speed = 20 m/s and convective clouds

Fig. 5-6 Comparison of corrected performance for different wind speeds

VI. Simplified Correction Algorithm

In section IV, when we chose the solutions for the initial wind direction assumption in the correction algorithm, we found that using previous-cell wind direction and speed is the best choice, as long as the wind retrieval algorithm has enough accuracy. If this is true, we can further simplify the correction algorithm. That is, we can use the previous-cell wind speed to estimate the sea-surface contribution to the AMSR measured T_b in the current cell. We can keep this estimation in the entire iteration and avoid using wind retrievals and wind direction. The benefits we get are the simplification of the correction algorithm and the reduced computer time needed to do the same number of iterations. Thus we simplified the correction algorithm by getting rid of the wind-retrieval part, which needs to evaluate the SASS model function and is quite time consuming.

The formulas used by the simplified algorithm are the same as for the original algorithm. The structure and the place it is located in the main SeaWinds Algorithm are also similar to the original algorithm. The procedure is as follows:

.Input the previous-cell wind speed as the current cell wind speed bias U_{bias}.

.Calculate the sea-surface contribution from U_{bias}.

.Calculate the excess temperature from the measured and estimated temperature.

.Use the cubic model to calculate the attenuation α.

.Perform the frequency scaling on α.

.Calculate the new sea-surface contribution considering the attenuation α.

.Go back and repeat.

These parts are plotted as plow chart as shown in Fig. 6-1, where the iteration is controlled by the improvement on the α (not on wind speed as used in original correction algorithm) and the maximum iteration number, which will be also different from the number used for the original correction algorithm.

Since the simplification was obtained by assuming the current wind speed is the same as the previous cell wind speed, we will not expect that the iteration to converge the exact solution. Moreover, the rate of convergence may be slower than for the original correction algorithm.

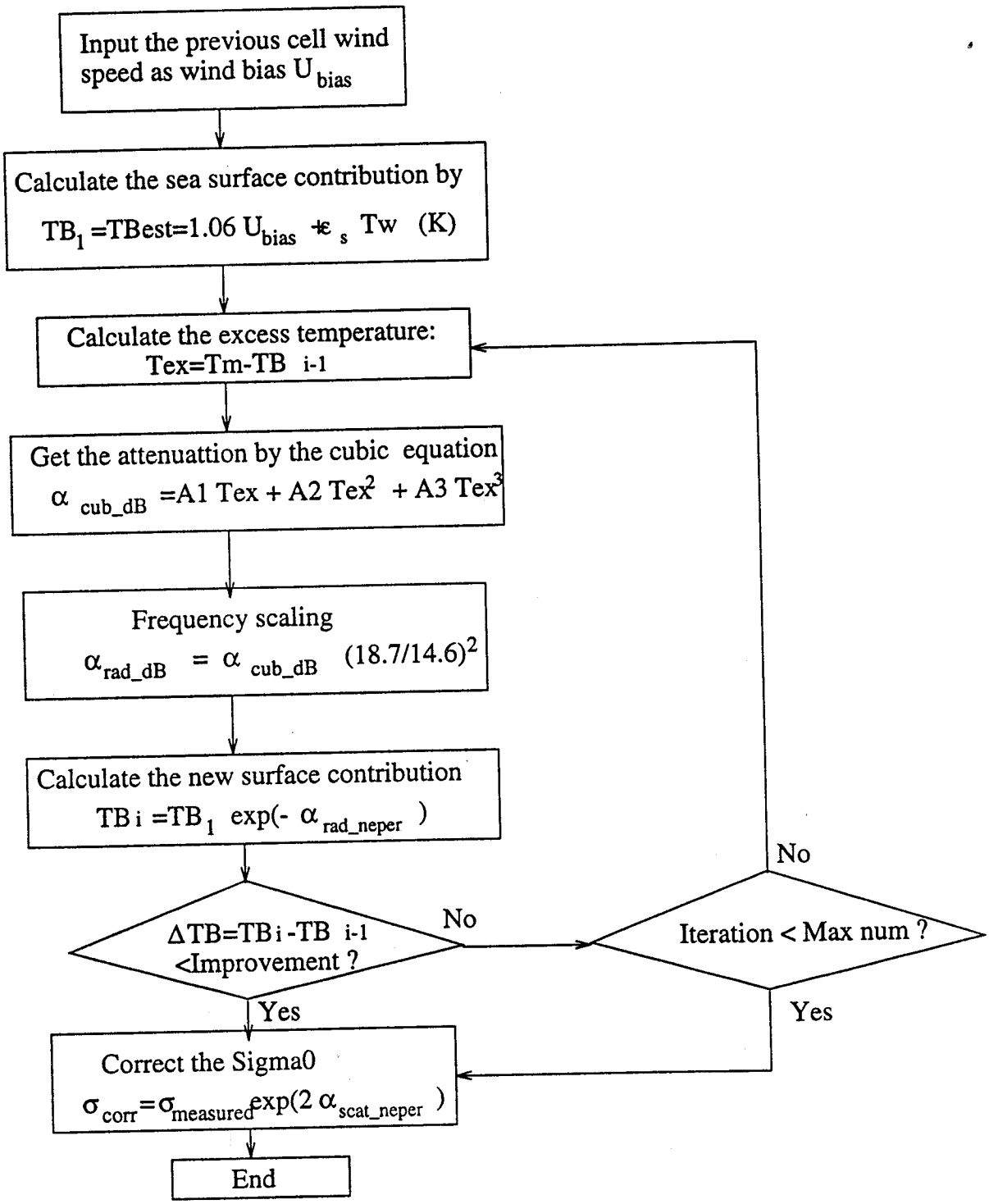

Fig.6-1 Block digram for the simplified correction algorithm

This means that, given the same error requirement, the simplified algorithm may need more iterations. However, the simplified algorithm needs less time for each iteration than the original algorithm, so the overall performance may be better than the original one.

To do simulation on the simplified correction algorithm, we first need to determine the maximum iteration number, just as for the original correction algorithm. Fig.6-1 shows the results for maximum iteration number used to achieved a specified level of error for both original correction algorithm and simplified algorithm. Comparing these two, we find that for the same excess temperature, the simplified algorithm needs a few more iterations to achieve the same level of performance for most cases, except for excess temperature near 140 K, in which the simplified algorithm needs many more iterations than the original one. To see the performance

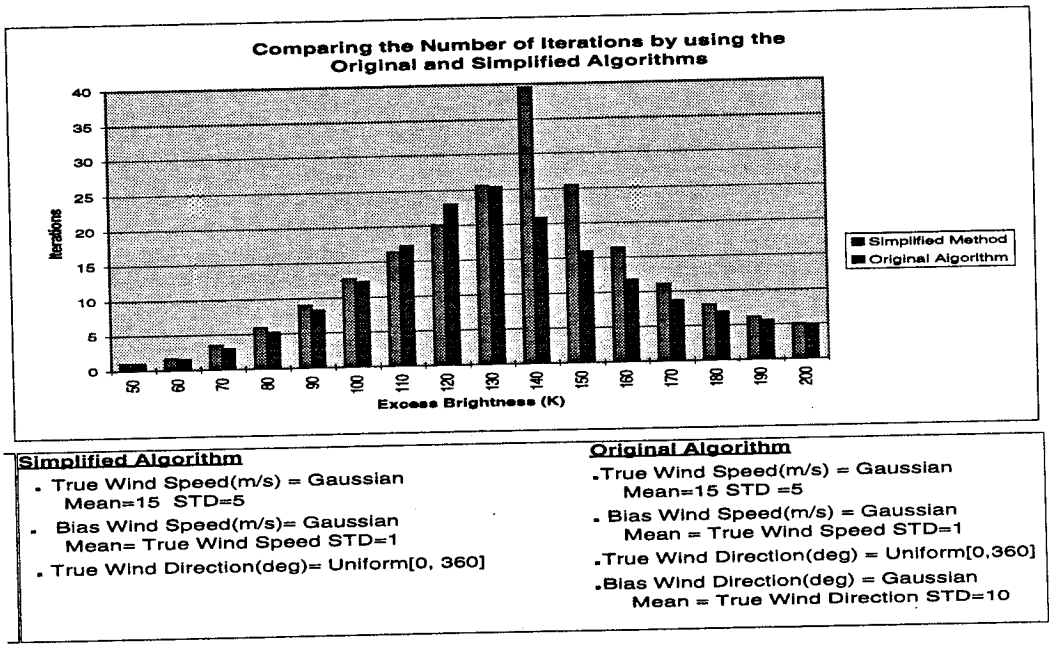

Fig.6-2 Comparison of the maximum iteration number by using the original correction algorithm and the simplified correction algorithm

difference, we simulate the correction by applying the simplified algorithm to the same situations we applied to the original correction algorithm. Fig. 6-3 to Fig. 6-5 show the simulation results.

The maximum iteration number is chosen from Fig. 6-1. Three segments for the measured temperature are used. The first segment is from 80 K to 140 K. If the measured temperature T_m fall inside this range , the maximum iteration number is chosen as 8. The second segment is from 140 K to 160 K for which the maximum iteration number is 25, a little more than that used for the original correction algorithm. The third segment is Tm larger than 160 K. We choose 10 as the maximum iteration number.

Fig. 6-3 shows the comparison of the correction performance of the simplified algorithm for two forms of clouds. As with the original algorithm, the simplified algorithm gives larger absolute improvement for stratiform clouds than for convective clouds. However, comparing Fig. 6-3 with Fig. 5-3, we see the correction performance of the simplified algorithm is somewhat poorer for stratiform clouds. For convective storms, there is no obvious difference. These results are consistent with Fig. 6-1.

Fig. 6-4 gives the correction performance of the simplified algorithm for different numbers of storms. Comparing it with the performance of original algorithm at the same situations, shown in Fig. 5-4, we can see that there is little difference between them. For convective clouds, the simplified algorithm gives nearly the same level of performance as the original algorithm. The maximum iteration number is also the same (for convective clouds, the measured T_m will mostly fall inside the first segment). That means that the simplified algorithm will need less time to get the same level of correction.

Fig. 6-5 shows the comparison of correction performance for different wind speeds. For stratiform clouds and wind speed 10 m/s, the simplified algorithm gets a little better performance than the original algorithm. However, for wind speed 20 m/s, it gives worse performance than the original algorithm. For convective storms at wind speed 10 m/s, the simplified algorithm is comparable with the original one. When wind speed is 20 m/s, its performance is a little bit worse than that of the original algorithm. From these results, we can see that ,when the wind speed is low, the simplified algorithm has similar performance to the original algorithm. For high wind speed, its performance is somewhat worse.

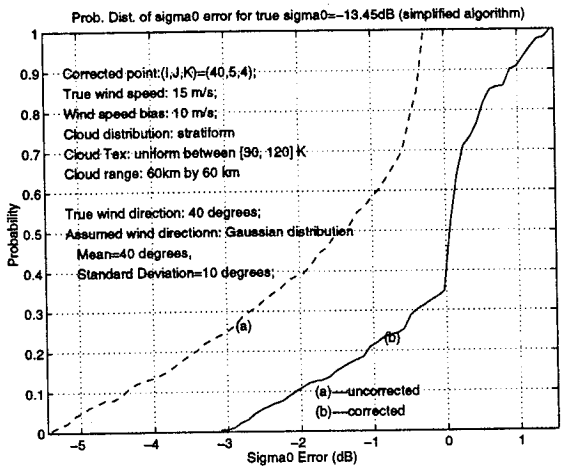

(a) σ_0 error for stratiform clouds

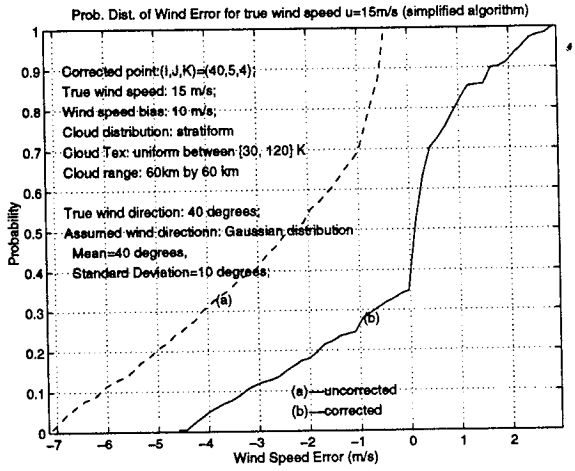

(b) Wind sped error for stratiform clouds

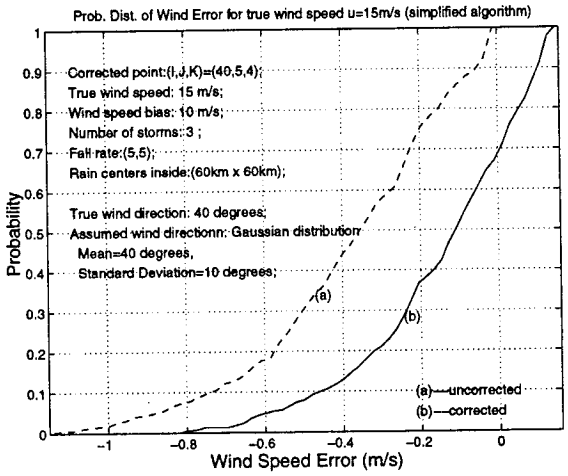

(c) σ_0 error for convective clouds

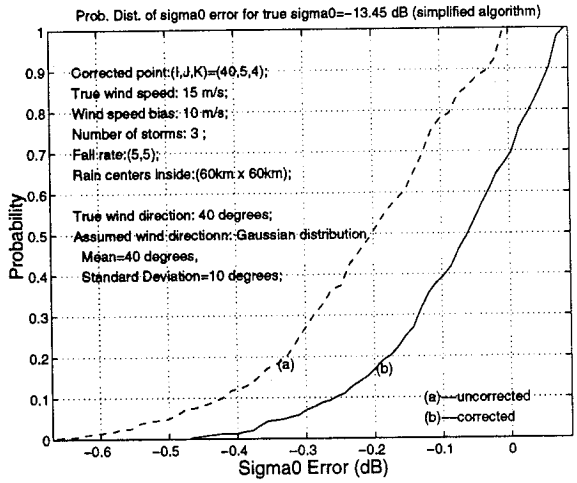

(d)Wind speed error for convective clouds

Fig. 6-3 Comparison of correction performance for two forms of clouds
(using the simplified correction algorithm)

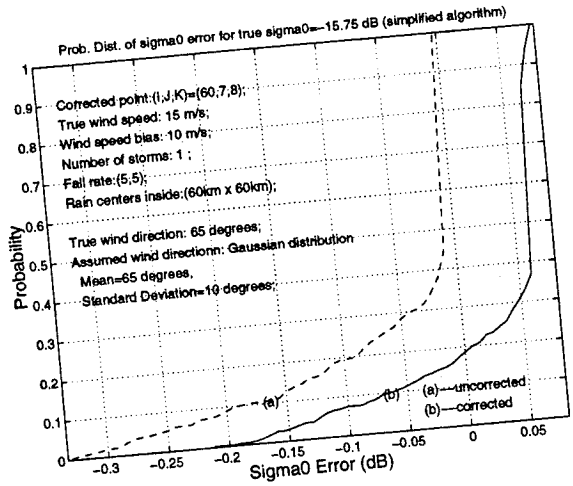

(a) One storm

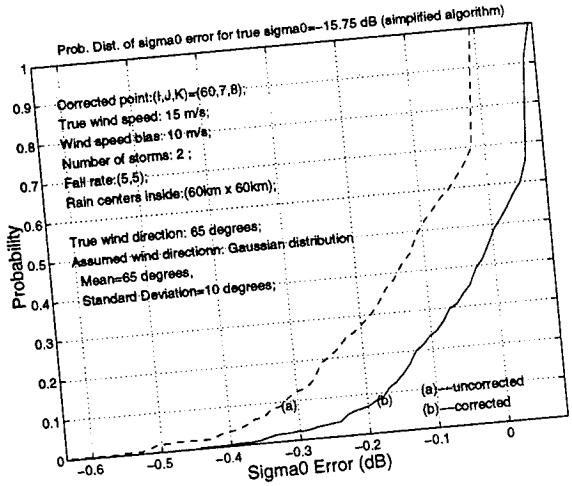

(b) Two storms

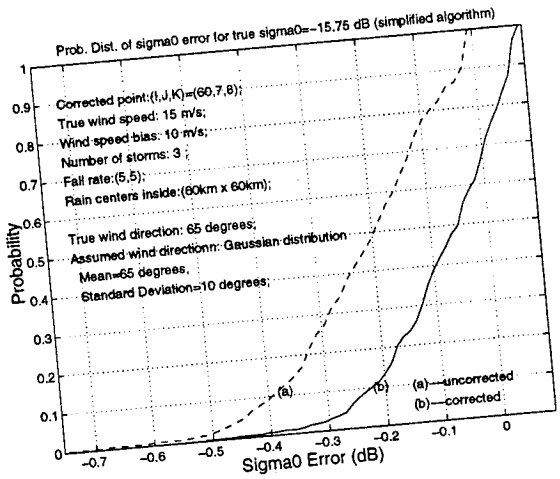

(c) Three storms

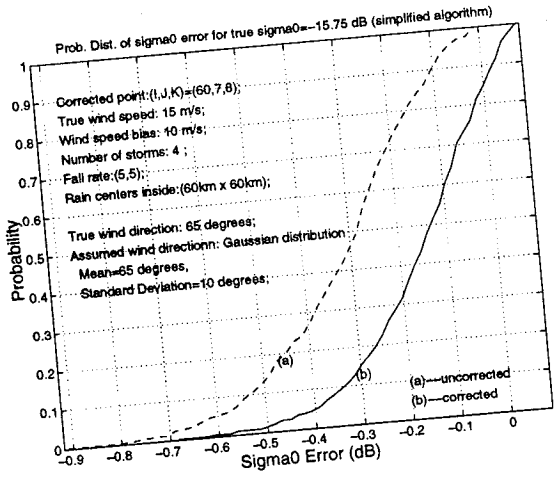

(d) Four storms

Fig. 6-4 Correction performance for different number of storms
(using the simplified correction algorithm)

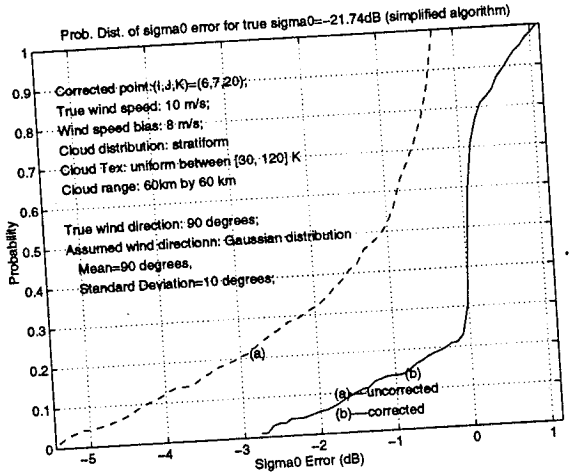

(a) Wind speed = 10 m/s
and stratiform clouds

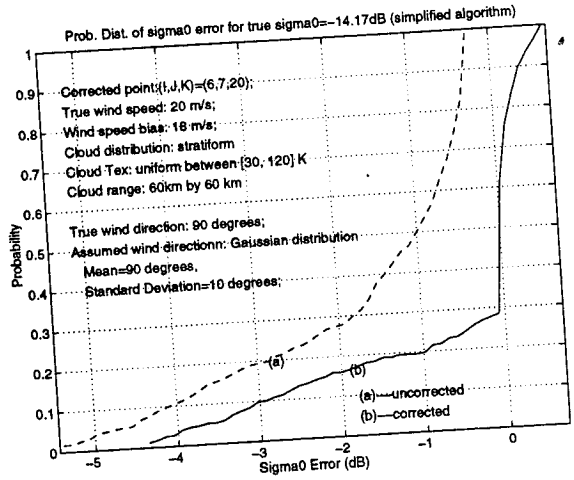

(b) Wind speed = 20 m/s
and stratiform clouds

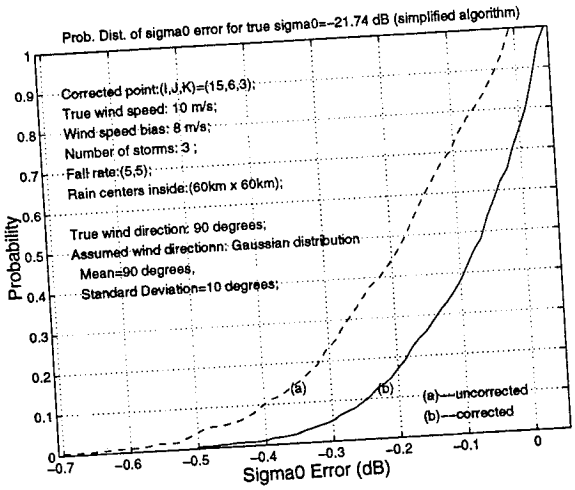

(c) Wind speed = 10 m/s
and convective clouds

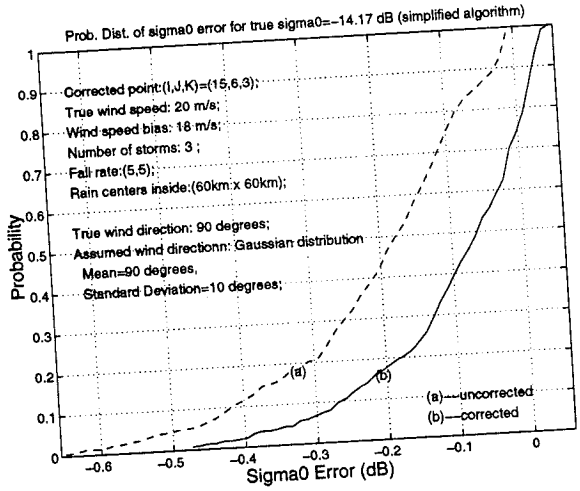

(d) Wind speed = 20 m/s
and convective clouds

Fig. 6-5 Comparison of corrected performance for different wind speeds
(using the simplified correction algorithm)

VII. Discussion and Conclusion

Seawinds scatterometer measurements will be in error when rain is present. Here we developed two approaches to correcting this error, at least in part, by using data from the AMSR radiometer. Simulations show that errors are small to begin with in systems of small convective storms, and the algorithms reduce these small errors considerably. When entire footprints of the scatterometer are filled with rain in stratiform systems, errors are much larger, and the value of the corrections is therefore greater.

Much of this report deals with a correction algorithm that uses scattering measurements to aid in application of the radiometer measurements. We propose three variations of this, but only two appear reasonable.

The basic problem in developing a correction is that the attenuation is related to the excess brightness temperature measured by the radiometer. To get the excess temperature from a measurement, one must know the surface brightness temperature, which depends on the wind speed. The algorithm iteratively solves for a wind-speed estimate and a surface brightness temperature. The latter is subtracted from the measured brightness temperature to obtain the excess temperature, which is then used to get the attenuation. At the end of the iterative process, the attenuation estimate is good enough so that it can be used to provide an estimate of the scattering that is significantly better than the raw (attenuated) measurement without correction.

The most desirable approach for the algorithm is to use the wind direction from the previous wind-vector cell. When the direction is known, one can use the scatterometer algorithm to obtain an estimate of the wind speed. This estimate then provides the information needed to get the surface brightness temperature. Since brightness temperature varies slowly with wind speed, the wind-speed estimate for this purpose need not be very accurate to arrive at a reasonable estimate of excess brightness temperature.

The less desirable approach is independent of the wind-vector output from the previous wind-vector cell. However, it depends on an assumed wind direction. The result is that the estimate of surface wind used to estimate surface brightness can have much larger errors than if a direction from a nearby region is used. Even so, the algorithm allows considerable improvement over no correction at all. Perhaps this method can be made better by using prevailing wind directions in different oceanic regions.

The rest of the report deals with an algorithm that does not use the local scattering measurement at all. Instead, it depends on a wind-speed estimate from the previous wind-vector cell. The algorithm uses this speed to determine the surface brightness temperature, from which the excess brightness temperature can be derived. It, too, is iterative. Although it requires more iterations for convergence than the scattering-based approach, each iteration is simpler, so it may well use less computer time to achieve a correction.

Both preferred methods depend on the assumption that the winds in the adjacent wind-vector cell are similar to the winds for the cell being corrected. Even choice of the wrong alias in the previous wind-vector cell should not cause a major error, since the wind speeds are similar in the aliases, and the direction should give a similar scattering coefficient in the model function, even if it is in the wrong quadrant. This assumption should be reasonable except when a front lies across or between the wind-vector cells or in a very tight cyclonic configuration. Hence, if at all possible, one of them should be used. The self-consistent method should be used only if the previous wind-vector-cell winds cannot be made available.

Monte Carlo simulations we performed show the kinds of errors before and after correction for both the convective-cell systems and the stratiform rains. For many convective systems the initial errors are so small that correction might not be necessary; however, the correction does give sizable error reductions. For stratiform situations, correction is mandatory if the wind measurements are to be reliable.

References

[1] R.K. Moore and W.J. Pierson," Measuring Sea State and Estimating Surface Winds from A Polar Orbiting Satellite", In Proc. Int. Symp. on EM Sensing of Earth from Satellites, Miami Beach, FL, 1966.

[2] F.M. Naderi, M.H. Freilich and D.G. Long,"Spaceborne Radar Measurement of Wind Velocity Over the Ocean-An Overview of the NSCAT Scatterometer System", Proc. of the IEEE, Vol.79, No.6, June 1991,pp.850-866.

[3] R.K. Moore and F.T. Ulaby, "The radar radiometer", Proc. of the IEEE,Vol.57, No.4, 1969,pp.587-590.

[4] R.K. Moore, etal.,"Evaluation of Atmospheric Attenuation From SMMR Brightness Temperature for the SEASAT Satellite Scatterometer", J. of Geophysical Research, Vol.87, No. C5,April 30,1982,pp.3337-3354.

[5] R.K. Moore, A.H. Chaudhry, and I.J. Birrer," Errors in Scatterometer-Radiometer Wind Measurement Due to Rain", IEEE J. Oceanic Eng., Vol.8, No. 1, 1983,pp.37-49.

[6] Kambhammettu, N., Radiometric Correction of Scatterometric Wind Measurements, RSL TR 9280-1, Septmember 1995.

[7] Jet Propulsion Laboratory, Science Algorithm Specification for SeaWinds, JPL, 4800 oak Grove Drive, Pasadena, California 91109, Oct. 10, 1995.

[8] F.T.Ulaby, R.K.Moore and A.K. Fung, Microwave Remote Sensing, Vol.III, Addision-Wesley Publishing Company,1986.

[9] C. Capsoni, etal., " Data and Theory for A New Model of the Horizontal Structure of Rain Cells for Propagation Applications", Radio Science, Vol.22, No.3, May/June, 1987,pp.395-403.